

Constructing hyperbolic polyhedra using Newton's Method

Roland K. W. Roeder ^{*}

February 2, 2008

Abstract

We demonstrate how to construct three-dimensional compact hyperbolic polyhedra using Newton's Method. Under the restriction that the dihedral angles are non-obtuse, Andreev's Theorem [8, 9] provides as necessary and sufficient conditions five classes of linear inequalities for the dihedral angles of a compact hyperbolic polyhedron realizing a given combinatorial structure C . Andreev's Theorem also shows that the resulting polyhedron is unique, up to hyperbolic isometry. Our construction uses Newton's method and a homotopy to explicitly follow the existence proof presented by Andreev, providing both a very clear illustration of proof of Andreev's Theorem as well as a convenient way to construct three-dimensional compact hyperbolic polyhedra having non-obtuse dihedral angles.

As an application, we construct compact hyperbolic polyhedra having dihedral angles that are (proper) integer sub-multiples of π , so that the group Γ generated by reflections in the faces is a discrete group of isometries of hyperbolic space. The quotient \mathbb{H}^3/Γ is hence a compact hyperbolic 3-orbifold, of which we study the hyperbolic volume and spectrum of closed geodesic lengths using SnapPea [58]. One consequence is a volume estimate for a "hyperelliptic" manifold considered in [35].

1 Introduction

Andreev's Theorem [8, 9] provides a complete characterization of compact hyperbolic polyhedra having non-obtuse dihedral angles. See also [25, 41] for an alternative exposition on the classical proof. Other approaches to Andreev's Theorem can be found by Rivin and Hodgson [37, 21], Thurston [51], Marden and Rodin [30], and Bowers and Stephenson [12]. In this paper we show that the classical proof from [8, 9, 25, 41] is constructive when combined with Newton's Method for solving nonlinear equations.

Combinatorial descriptions of hyperbolic polyhedra that are relevant to Andreev's Theorem fall into three classes, *simple*, *truncated*, and *compound*, all defined later in this section. The proof in [25, 41] provides an explicit continuous path in the space of polyhedra deforming a given simple polyhedron P to one of two which are easily constructed by hand: the N -faced prism Pr_N and the N -faced split prism D_N . We use Newton's method to follow such a path backwards deforming a computer realization of Pr_N or D_N to a computer realization of the desired polyhedron P . This technique, which has been well studied in the literature, is known as the homotopy method [6, 11, 47, 46, 48, 49, 7]. We illustrate the construction of simple polyhedra in Sections 2.5, 2.6, and 2.7.

A similar deformation, again using Newton's method, allows us to construct truncated polyhedra from simple polyhedra. We demonstrate this deformation in Section 2.8. In Section 2.9 we show how to construct a compound polyhedron as a gluing of two appropriate truncated polyhedra.

In this way, our program graphically illustrates Andreev's proof of existence for explicit examples. In fact, writing this program and working through Andreev's proof for some specific examples led to the detection an error in the proof of existence, which has been corrected in [25, 41].

^{*}rroeder@fields.utoronto.ca

[†]Partially supported by a U.S. National Defense Science and Engineering Fellowship and by the Fields Institute as a Jerrold E. Marsden postdoctoral fellow.

A further benefit of this program is the construction of polyhedra whose dihedral angles are proper integer sub-multiples of π . As a consequence of Poincaré's polyhedron theorem [20], the group Γ generated by reflections in the faces of such a polyhedron is a discrete group of isometries of hyperbolic space. The quotient \mathbb{H}^3/Γ is hence a compact hyperbolic 3-orbifold in which we study the hyperbolic volume and spectrum of closed geodesic lengths using SnapPea [58]. Such orbifolds and their covering manifolds have been studied extensively [29, 52, 35, 53, 17, 28, 36]. In fact the first example of a closed hyperbolic 3-manifold was obtained in this way in 1931 by Löbell [29]. One consequence of our study is a volume estimate for a “hyperelliptic” manifold considered in [35].

The reader should note that there are already excellent computer programs for experimentation with hyperbolic 3-manifolds. The program SnapPea [58] constructs hyperbolic structures on knot and link complements, as well as the hyperbolic Dehn surgeries on these complements. SnapPea provides for the computation of a variety of geometry invariants of the computed hyperbolic structure. (See also [4].) The program Snap [18, 14] provides a way of computing arithmetic invariants of hyperbolic manifolds. Both of these programs are quite easy to use and have allowed for vast levels of experimentation, including a nice census of low-volume hyperbolic manifolds and orbifolds.

The experimentation done in this paper with the hyperbolic orbifolds obtained from polyhedral reflection groups is very modest in comparison. However, it is an alternative way to construct hyperbolic structures on certain orbifolds (and, in the future, possibly on manifold covers of these orbifolds) in a way that these structures can nicely be studied by SnapPea (as well as Snap, and other software, in the future).

Let $E^{3,1}$ be \mathbb{R}^4 with the indefinite metric $\|\mathbf{x}\|^2 = -x_0^2 + x_1^2 + x_2^2 + x_3^2$. In this paper, we work in the hyperbolic space \mathbb{H}^3 given by the component of the subset of $E^{3,1}$ given by

$$\|\mathbf{x}\|^2 = -x_0^2 + x_1^2 + x_2^2 + x_3^2 = -1$$

having $x_0 > 0$, with the Riemannian metric induced by the indefinite metric

$$-dx_0^2 + dx_1^2 + dx_2^2 + dx_3^2.$$

The hyper-plane orthogonal to a vector $\mathbf{v} \in E^{3,1}$ intersects \mathbb{H}^3 if and only if $\langle \mathbf{v}, \mathbf{v} \rangle > 0$. Let $\mathbf{v} \in E^{3,1}$ be a vector with $\langle \mathbf{v}, \mathbf{v} \rangle > 0$, and define

$$P_{\mathbf{v}} = \{\mathbf{w} \in \mathbb{H}^3 | \langle \mathbf{w}, \mathbf{v} \rangle = 0\} \text{ and } H_{\mathbf{v}} = \{\mathbf{w} \in \mathbb{H}^3 | \langle \mathbf{w}, \mathbf{v} \rangle \leq 0\}$$

to be the hyperbolic plane orthogonal to \mathbf{v} and the corresponding closed half space.

If one normalizes $\langle \mathbf{v}, \mathbf{v} \rangle = 1$ and $\langle \mathbf{w}, \mathbf{w} \rangle = 1$ the planes $P_{\mathbf{v}}$ and $P_{\mathbf{w}}$ in \mathbb{H}^3 intersect in a line if and only if $\langle \mathbf{v}, \mathbf{w} \rangle^2 < 1$, in which case their dihedral angle is $\arccos(-\langle \mathbf{v}, \mathbf{w} \rangle)$. They intersect in a single point at infinity if and only if $\langle \mathbf{v}, \mathbf{w} \rangle^2 = 1$; in this case their dihedral angle is 0.

A *hyperbolic polyhedron* is an intersection

$$P = \bigcap_{i=0}^n H_{\mathbf{v}_i}$$

having non-empty interior.

We will often use the Poincaré ball model of hyperbolic space, given by the unit ball in \mathbb{R}^3 with the metric

$$4 \frac{dx_1^2 + dx_2^2 + dx_3^2}{(1 - \|\mathbf{x}\|^2)^2}$$

and the upper half-space model of hyperbolic space, given by the subset of \mathbb{R}^3 with $x_3 > 0$ equipped with the metric

$$\frac{dx_1^2 + dx_2^2 + dx_3^2}{x_3^2}.$$

Both of these models are isomorphic to \mathbb{H}^3 .

Hyperbolic planes in these models correspond to Euclidean hemispheres and Euclidean planes that intersect the boundary perpendicularly. Furthermore, these models are conformally correct, that is, the hyperbolic angle between a pair of such intersecting hyperbolic planes is exactly the Euclidean angle between the corresponding spheres or planes.

1.1 Combinatorial polyhedra and Andreev's Theorem

A compact hyperbolic polyhedron P is topologically a 3-dimensional ball, and its boundary a 2-sphere \mathbb{S}^2 . The face structure of P gives \mathbb{S}^2 the structure of a cell complex C whose faces correspond to the faces of P .

Considering only hyperbolic polyhedra with non-obtuse dihedral angles simplifies the combinatorics of any such C :

Proposition 1.1 (a) *A vertex of a non-obtuse hyperbolic polyhedron P is the intersection of exactly 3 faces.*

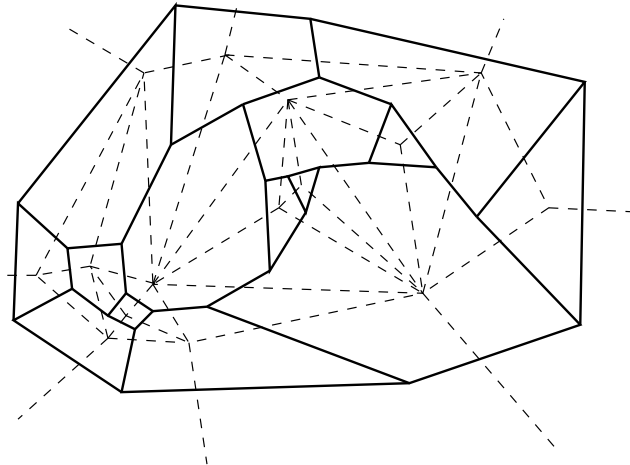
(b) *For such a P , we can compute the angles of the faces in terms of the dihedral angles; these angles are also $\leq \pi/2$.*

See [25, 41].

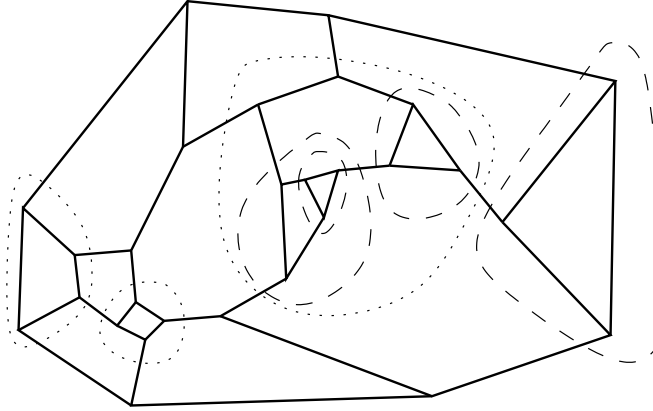
The fundamental axioms of incidence place the following, obvious, further restrictions on the complex C :

- Every edge of C belongs to exactly two faces.
- A non-empty intersection of two faces is either an edge or a vertex.
- Every face contains not fewer than three edges.

Any trivalent cell complex C on \mathbb{S}^2 that satisfies the three conditions above is an *abstract polyhedron*. Since C must be a trivalent cell complex on \mathbb{S}^2 , its dual, C^* , has only triangular faces and the three above conditions ensure that it is a simplicial complex on \mathbb{S}^2 . The figure below shows an abstract polyhedron C drawn in the plane (i.e. with one of the faces corresponding to the region outside of the figure.) The dual complex is also shown, in dashed lines.



We call a simple closed curve Γ formed of k edges of C^* a k -*circuit* and if all of the endpoints of the edges of C intersected by Γ are distinct, we call such a circuit a *prismatic k -circuit*. The figure below shows the same abstract polyhedron as above, except this time the prismatic 3-circuits are dashed, the prismatic 4-circuits are dotted, and the dual complex is not shown.



We say that a combinatorial polyhedron C is *simple* if it has no prismatic 3-circuits, *truncated* if C has prismatic 3-circuits and each surrounds on one side a single triangular face, and otherwise we call C *compound*. The combinatorial polyhedron shown in the two above diagrams is compound.

Theorem 1.2 Andreev's Theorem

Let C be an abstract polyhedron with more than 4 faces and suppose that non-obtuse angles \mathbf{a}_i are given corresponding to edge e_i of C . There is a compact hyperbolic polyhedron P whose faces realize C with dihedral angle \mathbf{a}_i at each edge e_i if and only if the following five conditions all hold:

1. For each edge e_i , $\mathbf{a}_i > 0$.
2. Whenever 3 distinct edges e_i, e_j, e_k meet at a vertex, $\mathbf{a}_i + \mathbf{a}_j + \mathbf{a}_k > \pi$.
3. Whenever Γ is a prismatic 3-circuit intersecting edges e_i, e_j, e_k , $\mathbf{a}_i + \mathbf{a}_j + \mathbf{a}_k < \pi$.
4. Whenever Γ is a prismatic 4-circuit intersecting edges e_i, e_j, e_k, e_l , then $\mathbf{a}_i + \mathbf{a}_j + \mathbf{a}_k + \mathbf{a}_l < 2\pi$.
5. Whenever there is a four sided face bounded by edges e_1, e_2, e_3 , and e_4 , enumerated successively, with edges $e_{12}, e_{23}, e_{34}, e_{41}$ entering the four vertices (edge e_{ij} connecting to the ends of e_i and e_j), then:

$$\mathbf{a}_1 + \mathbf{a}_3 + \mathbf{a}_{12} + \mathbf{a}_{23} + \mathbf{a}_{34} + \mathbf{a}_{41} < 3\pi, \quad \text{and}$$

$$\mathbf{a}_2 + \mathbf{a}_4 + \mathbf{a}_{12} + \mathbf{a}_{23} + \mathbf{a}_{34} + \mathbf{a}_{41} < 3\pi.$$

Furthermore, this polyhedron is unique up to isometries of \mathbb{H}^3 .

Corollary 1.3 If C is simple, i.e. has no prismatic 3-circuits, there exists a unique hyperbolic polyhedron realizing C with dihedral angles $2\pi/5$.

For a given C , let E be the number of edges of C . The subset of $(0, \pi/2]^E$ satisfying these linear inequalities will be called the *Andreev Polytope*, A_C . Since A_C is determined by linear inequalities, it is convex.

Andreev's restriction to non-obtuse dihedral angles is emphatically necessary to ensure that A_C be convex. Without this restriction, the corresponding space of dihedral angles, Δ_C , of compact (or finite

volume) hyperbolic polyhedra realizing a given C is not convex [15]. In fact, the recent work by Díaz [16] provides a detailed analysis of this space of dihedral angles Δ_C for the class of abstract polyhedra C obtained from the tetrahedron by successively truncating vertices. Her work nicely illustrate the types of non-linear conditions that are necessary in a complete analysis of the larger space of dihedral angles Δ_C .

The work of Rivin [39, 38] shows that the space of dihedral angles for ideal polyhedra forms a convex polytope, *without the restriction to non-obtuse angles*. (See also [19].)

Notice also that the hypothesis that the number of faces is greater than four is also necessary because the space of non-obtuse dihedral angles for compact tetrahedra is not convex [42]. Conditions (1-5) remain necessary conditions for compact tetrahedra, but they are no longer sufficient.

Bao and Bonahon [10] prove a similar classification theorem for hyperideal polyhedra. Finally, the papers of Vinberg on discrete groups of reflections in hyperbolic space [5, 54, 55, 56, 57] are also closely related, as well as the work of Bennett and Luo [13] and Schlenker [43, 44, 45].

Much attention has been focused on Andreev's Theorem from the viewpoint of circle packings and circle patterns. Given a polyhedron P in the upper half-space model of \mathbb{H}^3 , the planes supporting the faces of P intersect the boundary at infinity $x_3 = 0$ in a pattern of circles (and straight lines) each with an orientation specifying "on which side" is the polyhedron P . Similarly, from such a pattern of circles and orientations one can re-construct a polyhedron P .

The works of Thurston [51], Marden and Rodin [30], and Bowers and Stephenson [12] all follow this approach to Andreev's Theorem. In fact, there is a beautiful computer program known as Circlepack [50], written by Ken Stephenson, that computes circle packings and patterns of circles with specified angles of overlap. All of the proofs from this point of view use the conformal structure of the Riemann sphere $\hat{\mathbb{C}} = \partial_\infty \mathbb{H}^3$ and use the correspondence between conformal automorphisms of $\hat{\mathbb{C}}$ with isometries of \mathbb{H}^3 .

Instead of using the conformal structure on $\partial_\infty \mathbb{H}^3$, in this paper we will work specifically with the metric structure of \mathbb{H}^3 . (However, there is certainly some significant overlap with the results in [51, 30, 12] and with the capabilities of the computer program CirclePack [50].)

We will now explain the implementation of a computer program whose input is the combinatorial polyhedron C and a dihedral angle vector $\mathbf{a} \in A_C$ and whose output is a hyperbolic polyhedron realizing the pair (C, \mathbf{a}) .

1.2 An example

The following figure shows an explicit example of the data (C, \mathbf{a}) and the resulting polyhedron displayed in the conformal ball model using the computer program Geomview [3].

1.3 Outline of the proof of Andreev's Theorem

In this section, we recall the major steps from the proof of Andreev's Theorem that were presented in [25, 41].

Let C be a trivalent abstract polyhedron with N faces. We say that a hyperbolic polyhedron $P \subset \mathbb{H}^3$ *realizes* C if there is a cellular homeomorphism from C to ∂P (i.e., a homeomorphism mapping faces of C to faces of P , edges of C to edges of P , and vertices of C to vertices of P). We will call each isotopy class of cellular homeomorphisms $\phi : C \rightarrow \partial P$ a *marking* on P .

We defined \mathcal{P}_C to be the set of pairs (P, ϕ) so that ϕ is a marking with the equivalence relation that $(P, \phi) \sim (P', \phi')$ if there exists an automorphism $\rho : \mathbb{H}^3 \rightarrow \mathbb{H}^3$ such that $\rho(P) = P'$, and both ϕ' and $\rho \circ \phi$ represent the same marking on P' .

Proposition 1.4 *The space \mathcal{P}_C is a manifold of dimension $3N - 6$ (perhaps empty).*

The proof is relatively standard and can be found in [25, 41].

Since the edge graph of C is trivalent, the number E of edges of C is the same as the dimension of \mathcal{P}_C . Given any $P \in \mathcal{P}_C$, let $\alpha(P) = (\mathbf{a}_1, \mathbf{a}_2, \mathbf{a}_3, \dots)$ be the E -tuple consisting of the dihedral angles of P

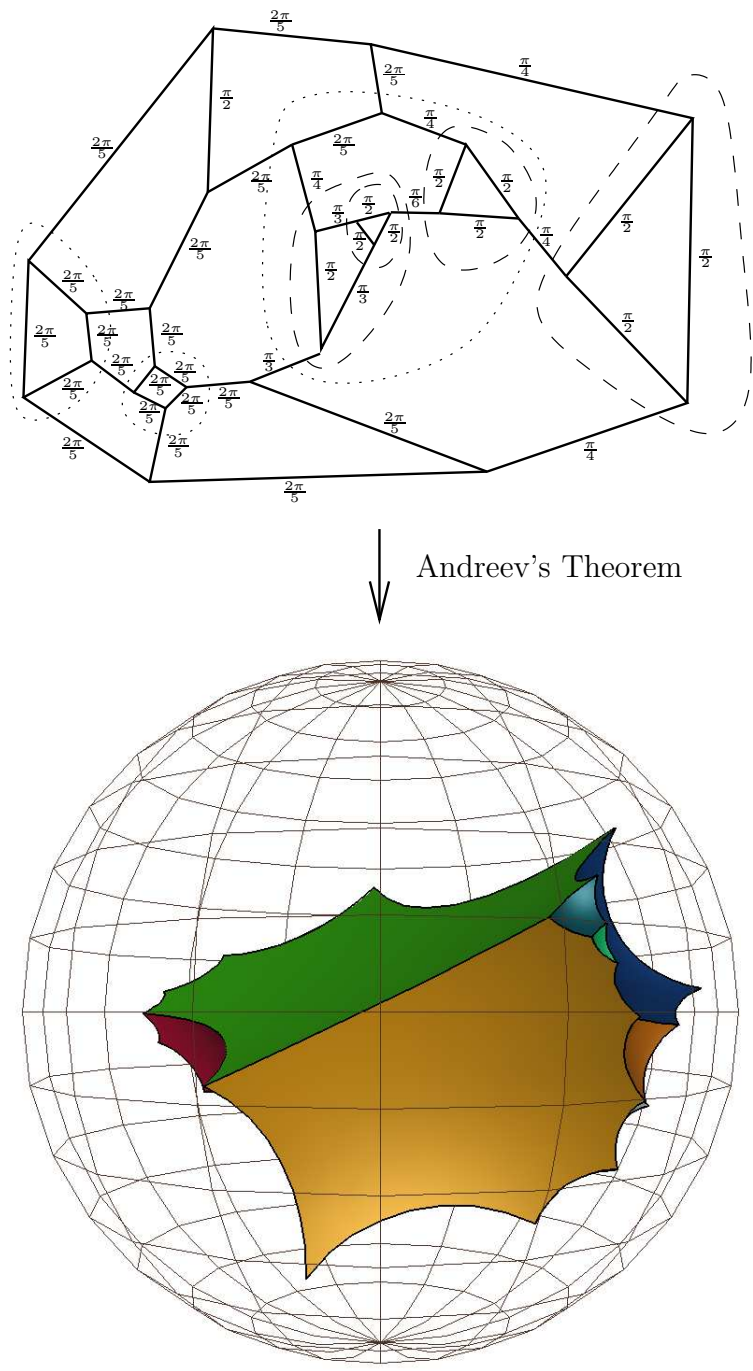


Figure 1:

at each edge (according to some fixed numbering of the edges of C). This map α is obviously continuous with respect to the topology on \mathcal{P}_C , which it inherits from its manifold structure.

We let \mathcal{P}_C^0 be the subset of \mathcal{P}_C consisting of polyhedra with non-obtuse dihedral angles. To establish Andreev's Theorem, we proved the following statement:

Theorem 1.5 *For every abstract polyhedron C having more than four faces, the mapping $\alpha : \mathcal{P}_C^0 \rightarrow A_C$ is a homeomorphism.*

There were two major steps:

Proposition 1.6 *If $\mathcal{P}_C^0 \neq \emptyset$, then $\alpha : \mathcal{P}_C^0 \rightarrow A_C$ is a homeomorphism.*

We checked that $\alpha(\mathcal{P}_C^0) \subset A_C$ by showing that conditions (1)-(5) are necessary. There is an open subset $\mathcal{P}_C^1 \subset \mathcal{P}_C$ containing \mathcal{P}_C^0 on which one can prove that $\alpha : \mathcal{P}_C^1 \rightarrow \mathbb{R}^E$ is injective, using a modification of Cauchy's rigidity for Euclidean polyhedra. This gives the uniqueness part of Andreev's Theorem. Using invariance of domain, it also gives that $\alpha : \mathcal{P}_C^1 \rightarrow \mathbb{R}^E$ is a local homeomorphism. Because $\mathcal{P}_C^0 \subset \mathcal{P}_C^1$, α restricted to \mathcal{P}_C^0 is a local homeomorphism, as well.

We then showed that $\alpha : \mathcal{P}_C^0 \rightarrow A_C$ is proper, which amounts to showing that if a sequence of polyhedra P_i in \mathcal{P}_C^0 degenerate (i.e. leave \mathcal{P}_C^0) then the sequence $\alpha(P_i)$ tends to ∂A_C . The fact that $\alpha : \mathcal{P}_C^0 \rightarrow A_C$ is a proper local homeomorphism was sufficient to show that $\alpha(\mathcal{P}_C^0)$ is open and closed in A_C .

Proposition 1.7 *If $A_C \neq \emptyset$, then $\mathcal{P}_C^0 \neq \emptyset$.*

The second step was much more difficult because for each C with non-empty A_C one needed to construct some polyhedron realizing C (with non-obtuse dihedral angles). In fact the proof of Proposition 1.7 outlines a scheme for how to construct a polyhedron realizing C . The remainder of this paper outlines how to follow this scheme explicitly on the computer using Newton's Method and a homotopy method.

2 A method for constructing Andreev polyhedra

2.1 Representing polyhedra on the computer

All the constructions of polyhedra done in this paper are using Matlab [1] or the Free Software Foundation alternative Octave [2], and all of the polyhedra are displayed in Geomview [3]. When doing calculations, we represent a hyperbolic polyhedron P having N faces by specifying N outward pointing normal vectors vectors $\mathbf{v}_1, \dots, \mathbf{v}_N$ each with $\langle \mathbf{v}_i, \mathbf{v}_i \rangle = 1$, so that $P = \bigcap_{i=1}^n H_{v_i}$.

Although such a list of N vectors is sufficient to specify P , in order to avoid repeated computation of the combinatorial structure of P from these vectors we additionally specify the adjacency matrix and a list of all plane triples meeting at a vertex. These three items are described in a Matlab struct P , with $P.faces$, $P.adjacency$, and $P.vert$ holding the data mentioned above, respectively.

For example, the data for the polyhedron shown in Section 1.2 is stored in Matlab as:

```
New_poly =
    vert: [28x3 double]
    faces: [16x4 double]
    adjacency: [16x16 double]

New_poly.faces =
 36.5078 -10.7624 -0.3090 -34.8983
 4.9237 -1.5291 -1.2342 -4.6240
-0.0000 0.8660 -0.5000 -0.0000
 4.5134 -2.1988 -2.3943 -3.2868
 2.7290 -1.9854 -0.3091 -2.1000
13.3691 -5.0338 -0.3090 -12.4216
65.0863 -19.6363 -2.7939 -61.9987
35.9576 -9.6209 -1.5515 -34.6262
51.5713 -13.3145 -0.3090 -49.8320
 5.8378 -0.5352 -0.3090 -5.8905
-0.0000 0.0000 1.0000 0.0000

New_poly.adjacency =
 1 0 0 0 1 1 1 1 1 0 1 0 0 0 0 0
 0 1 1 1 1 1 1 0 1 0 0 1 0 0 0 0
 0 1 1 1 0 0 0 0 0 1 1 1 1 1 1 1
 0 1 1 1 1 0 0 0 0 0 0 1 1 1 1 0
 0 1 0 1 1 1 0 0 0 0 0 1 1 0 0 0
 1 1 0 0 1 1 1 0 0 0 0 1 0 0 0 0
 1 1 0 0 0 1 1 1 0 0 0 0 0 0 0 0
 1 1 0 0 0 0 1 1 1 0 0 0 0 0 0 0
 1 1 0 0 0 0 0 1 1 1 0 0 0 0 0 0
 1 1 0 0 0 0 0 0 1 1 1 0 0 0 0 0
 1 1 0 0 0 0 0 0 0 1 1 1 0 0 0 0
 1 1 0 0 0 0 0 0 0 0 1 1 1 0 0 0
 1 1 0 0 0 0 0 0 0 0 0 1 1 1 0 0
 0 1 1 0 0 0 0 0 0 0 1 1 1 1 0 0
```

```

1   0   1   0   1   1   0   0   1   1   1   1   0   0   1   0
0   0   1   1   0   0   0   0   0   0   1   0   1   0   1   1
0   1   1   1   0   0   0   0   0   0   0   0   1   0   0   0
0   0   1   1   0   0   0   0   0   0   0   1   0   1   0   0
0   0   1   0   0   0   0   0   0   0   1   1   0   0   1   1
0   0   1   0   0   0   0   0   0   0   1   0   1   0   1   1
New_poly.vert =
3   4   14
6   5   11
4   12   5
12   5   11
1   6   7
1   7   8
1   8   9
1   9   11
10   9   11
1   6   11
2   3   13
2   4   5
2   5   6
2   6   7
2   7   8
2   8   10
2   9   10
2   10   3
11   10   3
2   4   13
3   4   13
3   12   14
3   12   14
4   12   14
11   3   15
11   12   15
3   12   16
3   15   16
12   15   16

```

We display the polyhedra in Geomview using the hyperbolic mode and specifying the conformal ball model. The file format most convenient for our use is the Object File Format, “New_poly.off.” The first line of an Object format file specifies the number of vertices, the number of faces, and the number of edges of P in that order: num_vert num_faces num_edges.

The next block of data is a list of the coordinates of vertices as points in the unit ball. (In fact, these are the coordinates of points in the Projective Model for \mathbb{H}^3 , not the Poincaré ball model which we describe in the introduction.) The last block of data is a list of the faces with each face given by $\text{vertex}_1 \text{ vertex}_2 \dots \text{vertex}_n$ colorspec, where the faces is spanned by $\text{vertex}_1 \text{ vertex}_2 \dots \text{vertex}_n$ and colorspec is an integer telling Geomview what color to assign to the face.

```

28 16 42          0.301741 0.507113 -0.798909
0.093414 0.626297 -0.759378          -0.023848 -0.005394 -0.995609
0.668701 -0.423986 0.508660          0.158629 -0.006953 -0.985479
0.480895 0.480927 -0.729094          0.065661 0.192695 -0.976218
0.533074 -0.046431 -0.835831          0.028183 0.094604 -0.992919
0.000602 -0.321164 0.944739          0.091162 0.094314 -0.989423
-0.109909 -0.298793 0.946284
-0.257482 -0.413626 0.871178
-0.241811 -0.517345 0.817366
-0.394737 -0.502851 0.762029
0.039860 -0.522084 0.841280
-0.198257 0.894806 -0.304826
0.473945 0.834475 -0.252208
0.632626 0.016126 0.705772
0.030462 -0.199457 0.975695
-0.112637 -0.193119 0.972142
-0.373893 -0.377706 0.844031
-0.376723 -0.130280 0.905450
-0.802208 0.544817 0.123196
-0.869841 -0.223571 -0.241933
0.160888 0.910483 -0.333052
0.007468 0.802257 -0.570580
0.104068 0.367146 -0.917226

```

Something is lacking when viewing the polyhedra displayed in the two-dimensional images shown in this paper. To alleviate this difficulty, the Matlab and OFF files associated to each polyhedron that is constructed in this paper are included as supplementary materials on the website of Experimental Mathematics. See the website [3] for full details on the use of Geomview.

2.2 The desired polyhedron as a solution to $4N$ quadratic equations in $4N$ unknowns

The proof of Andreev's Theorem gives that $\alpha_C : \mathcal{P}_C^0 \rightarrow A_C$ is a homeomorphism, so the problem of constructing a polyhedron P realizing (C, \mathbf{a}) can be expressed as the problem of finding a solution P to the equation $\alpha_C(P) = \mathbf{a}$.

Instead of working in \mathcal{P}_C^0 , we write the desired polyhedron as a solution of a system of $4N$ quadratic equations in $4N$ variables, where N is the number of faces of C . Our solution is N vectors $v_1, \dots, v_N \in E^{3,1}$ satisfying

- $\langle v_i, v_i \rangle = 1$ and

- $\langle v_j, v_j \rangle = -\cos(\mathbf{a}_{i,j})$ if faces i and j are adjacent in C and their common edge is assigned dihedral angle $\mathbf{a}_{i,j}$.

These equations impose $E + N$ conditions on $4N$ variables, where C has N faces and E edges.

As mentioned in Section 1.3, we have $E = 3N - 6$, so we have imposed $4N - 6$ conditions on $4N$ variables. We impose 6 additional conditions in order to have the same number of equations and unknowns. We normalize by requiring that a chosen vector v_i perpendicular to one of the faces agree with some given v (where v is chosen so that $\langle v, v \rangle = 1$.) We then require that one of the vertices on the face perpendicular to v_i is at a given point w in the plane P_v and that a vertex adjacent to this vertex be on a given line l in P_v through w . One can check that these normalizations provide 3, 2, and 1 additional equations respectively. (Notice that the six equations for this normalization are each linear.) We denote the normalization by a triple (v, w, l) .

We denote the resulting quadratic map by $F_{C,(v,w,l)} : \mathbb{R}^{4N} \rightarrow \mathbb{R}^{4N}$. Typically we will only mention the normalization when necessary. We denote the conditions described above for the right hand side of the equations $F(x) = y$ as $(\mathbf{a}, 0)$, where the \mathbf{a} from this pair is shorthand for the conditions $\langle v_i, v_i \rangle = 1$ and $\langle v_j, v_j \rangle = -\cos(\alpha_{i,j})$ if faces i and j are adjacent in C , and the 0 represents the fact that the normalization (v, w, l) is satisfied.

Andreev's Theorem asserts that if $\mathbf{a} \in A_C$, there is a real solution to $F_{C,(v,w,l)}(x) = (\mathbf{a}, 0)$ corresponding to N vectors $\mathbf{v}_1, \dots, \mathbf{v}_N$ in $E^{3,1}$ so that $P = \bigcap_{i=0}^n H_{\mathbf{v}_i}$ realizes the pair (C, \mathbf{a}) .

There are many sensible ways to numerically solve a system of quadratic equations in the same number of equations as unknowns. These include the pre-packaged non-linear solvers in Matlab, Maple, and Mathematica, Newton's Method, as well as Groebner basis techniques and fancier quadratically constrained solvers.

The difficulty is that with $4N$ quadratic equations in $4N$ unknowns, Bezout's Theorem states that there will typically be $16N^2$ solutions. On their own, these solvers cannot easily be adapted to find the specific solution corresponding to a convex polyhedron, without first finding all solutions (or at least all real solutions) and then examining each solution to check if it corresponds to the desired polyhedron. Since some solutions may be much harder to find than others, one could spend significant computation times pursuing solutions that aren't of interest.

One way to ensure that the solution does correspond to a compact convex polyhedron is to use an iterative method, like Newton's Method, for which an initial condition that is sufficiently close to a given solution is guaranteed to converge to that root, in combination with a homotopy that guarantees that the nearest root is always the root that corresponds to a compact convex polyhedron. This is our approach, which we describe in greater detail in the next few sections of the paper. We are not entirely sure that this method is faster than finding all of the roots with "brute force" and then checking each solution to see if it is the desired one, but our approach has the additional benefit that it explicitly follows Andreev's proof of existence, providing insight into how this proof works for specific examples.

2.3 Newton's Method and Homotopy methods

Given two vector spaces V and W of the same dimension and a mapping $F : V \rightarrow W$, the associated Newton map $N_F : V \rightarrow V$ is given by the formula

$$N_F(\mathbf{x}) = \mathbf{x} - [DF(\mathbf{x})]^{-1}(F(\mathbf{x})). \quad (1)$$

If the roots of F are non-degenerate, i.e. $DF(r_i)$ is invertible for each root r_i of F , then the roots of F corresponds bijectively to super-attracting fixed points of N_F .

Kantorovich's Theorem [27] gives a precise lower bound on the size of the basin of attraction for a root.

Theorem 2.1 (Kantorovich's Theorem). *Let \mathbf{a}_0 be a point in \mathbb{R}^n , U an open neighborhood of \mathbf{a}_0 in \mathbb{R}^n , and $F : U \rightarrow \mathbb{R}^n$ a differentiable mapping with $[DF(\mathbf{a}_0)]$ invertible.*

Let U_0 be the open ball of radius $\|DF(\mathbf{a}_0)\|^{-1}F(\mathbf{a}_0)$ centered at $\mathbf{a}_1 = N_F(\mathbf{a}_0)$. If $U_0 \subset U$ and $[DF(\mathbf{x})]$ satisfies the Lipschitz condition $\|DF(\mathbf{u}_1) - DF(\mathbf{u}_2)\| \leq M|\mathbf{u}_1 - \mathbf{u}_2|$ for all $\mathbf{u}_1, \mathbf{u}_2 \in U_0$, and if the inequality

$$|F(\mathbf{a}_0)| \cdot \|DF(\mathbf{a}_0)\|^{-1}M \leq \frac{1}{2} \quad (2)$$

is satisfied, then the equation $F(\mathbf{x}) = 0$ has a unique solution in U_0 , and Newton's Method with initial guess \mathbf{a}_0 converges to it.

For a proof of Kantorovich's Theorem see [24] or the original source [27].

While the dynamics near a fixed point can be easily understood by Kantorovich's Theorem, the global dynamics of Newton's Method can be very complicated, with loci of indeterminacy, and critical curves where DN is not injective. In fact, the dynamics of Newton's method to solve for the common roots of a pair of quadratic polynomials in \mathbb{C}^2 is a field of active research [23, 40]. We expect that the global dynamics of the Newton map to solve $F_{C,(v,w,l)}(x) = (\mathbf{a}, 0)$ is even significantly more complicated than those in [23, 40]. In particular, we have no reason to expect that a general initial condition in R^{4N} will converge under iteration of N_F to any solution of $F_{C,(v,w,l)}(x) = (\mathbf{a}, 0)$ nor to the specific solution representing a convex compact polyhedron P .

An approach that can sometimes be used to avoid the difficulties with the global dynamics of Newton's Method is the homotopy method. Suppose that you want to solve $g(x) = y$. The idea is to replace this equation by a family that depends continuously on a single variable:

$$g_t(x_t) = y_t$$

so that g_1 is the same function as g and $y_1 = y$, while $g_0(x) = y_0$ is an equation for which you already know a solution x_0 .

Choose k points $0 = t_1, t_2, \dots, t_k = 1$. If k is sufficiently large, then x_{t_1} may be in the basin of attraction of the Newton's method for $f_{t_2}(x) = y_{t_2}$. In this case, you can solve for x_{t_2} and can attempt to solve for x_{t_3} using Newton's Method for $f_{t_3}(x) = y_{t_3}$ with initial condition x_{t_2} . Repeating this procedure, if possible, leads to the solution $x_1 = x_{t_k}$.

While this is obviously a very powerful method, there are many difficulties choosing appropriate paths $g_t(x_t) = y_t$ and appropriate subdivisions $0 = t_1, t_2, \dots, t_k = 1$. It is necessary to check that the conditions for Kantorovich's Theorem are satisfied by x_{t_j} for the equation $f_{t_{j+1}}(x) = y_{t_{j+1}}$. The biggest difficulty is to avoid the situation where the derivative $\frac{\partial}{\partial x} f_t$ is singular for some t . Such points are described as being in the *discriminant variety* and choosing paths that avoid the discriminant variety is a big program of research. These difficulties are discussed extensively by many authors including Shub and Smale in [11, 6, 47, 46, 48, 49, 7].

The proof of Andreev's Theorem in [25, 41] provides an explicit path that we can use for a homotopy method to construct any simple polyhedron P as a continuous deformation of either the prism Pr_N or the split prism D_N , both of which can be easily constructed "by hand". We will use this path for our homotopy method: repeatedly using a polyhedron realizing a point on the path as initial condition and solving for a polyhedron slightly further on the path, chosen so that the dynamics of Newton's method converges to the correct solution of F .

With a similar path we can use the homotopy method again to construct any truncated polyhedron for which $A_C \neq \emptyset$. We take a continuous deformation of a simple polyhedron until the vertices to be truncated pass $\partial_\infty \mathbb{H}^3$, and then add a finite number of additional triangular faces intersecting the appropriate triples of faces perpendicularly. Compound polyhedra are then constructed as gluings of a finite number of truncated polyhedra.

Proposition 2.2 *The quadratic equation F has a uniform Lipschitz constant on R^{4N} depending only on the combinatorics C .*

Proof: The proof is merely the observation that F is quadratic so each of the second derivatives are constant. \square

While we have checked that F is Lipschitz, we make no effort to bound the norm of the derivative $[DF]$ away from zero (hence avoiding the discriminant variety). In fact, for a typical problem this is very hard to do. Instead, we merely try the homotopy method with the path mentioned in the preceding paragraph and we show that the method works for all of the constructions that we attempt. It may be interesting to provide a more rigorous basis for our use of Newton's Method and the current choice of path.

2.4 Deforming a given polyhedron using Newton's Method

Given a polyhedron P realizing C with dihedral angles $\mathbf{a} \in A_C$, it is easy to use Newton's method to deform P into a new polyhedron P' having any other angles $\mathbf{a}' \in A_C$. Since A_C is a convex polytope, choose the line segment between \mathbf{a} and \mathbf{a}' and subdivide this segment into K equally distributed points $\mathbf{a} = \mathbf{a}^0, \mathbf{a}^1, \mathbf{a}^2, \dots, \mathbf{a}^{K-1} = \mathbf{a}'$. Then we use Newton's method with initial condition corresponding to P to solve for a polyhedron P_1 with dihedral angles \mathbf{a}^1 . We then repeat, using P_1 as initial condition for Newton's method to solve for a polyhedron P_2 with dihedral angles \mathbf{a}^2 , and continue until reaching P' realizing \mathbf{a}' . If the homotopy method has worked, then each step of Newton's method converges; otherwise we can try a larger number of subdivisions K , or attempt to check if the path has hit the discriminant variety.

In all of the calculations within this paper, when deforming the angles of a given polyhedron P within A_C , we use K between 100 and 300 subdivisions, although this is sometimes a significant overkill.

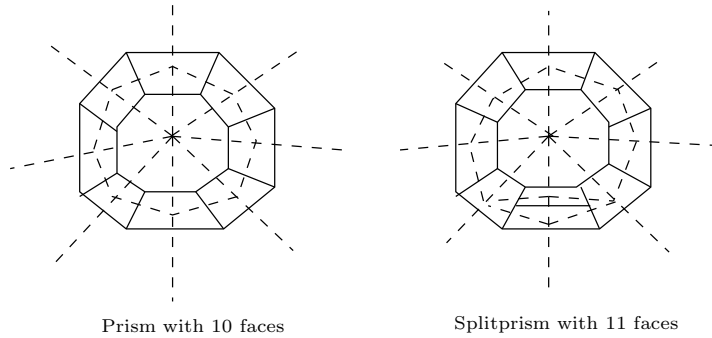
We consider it sufficient to show how to use Newton's method to construct some polyhedron P with non-obtuse dihedral angles for every C that has $A_C \neq \emptyset$. From this P one can construct any other $P' \in \mathcal{P}_C^0$ using the deformation described above. (This ease with which one can deform the angles of a given polyhedron is an additional benefit of our homotopy method.)

In the next sections we will see how to connect individual paths in A_{C_1}, \dots, A_{C_k} so as to construct compact polyhedra realizing C_1 as a sequence of deformations of a compact polyhedron realizing C_k .

2.5 Simple polyhedra and Whitehead moves

Recall that if C is simple then $(\frac{2\pi}{5}, \dots, \frac{2\pi}{5}) \in A_C$. The goal of this section and the following is to demonstrate the construction of a polyhedron P realizing any simple C with these dihedral angles.

Andreev's Theorem provides a sequence of elementary changes (Whitehead moves) to the reducing the combinatorics C to one of two the combinatorial polyhedra D_N or Pr_N depicted below.



In this section we show how to create polyhedra realizing D_N and Pr_N and how to do the Whitehead moves using Newton's method.

Lemma 2.3 Let Pr_N and D_N be the abstract polyhedra corresponding to the N -faced prism and the N -faced “split prism”, as illustrated below. If $N > 4$, $\mathcal{P}_{Pr_N}^0$ is nonempty and if $N > 7$, $\mathcal{P}_{D_N}^0$ is nonempty.

Construction: Construct a regular polygon with $N - 2$ sides in the disc model for \mathbb{H}^2 . ($N - 2 \geq 3$, since $N \geq 5$.) We can do this with the angles arbitrarily small. Now view \mathbb{H}^2 as the equatorial plane of \mathbb{H}^3 , and consider the hyperbolic planes perpendicular to the equatorial plane containing the sides of the polygon. In Euclidean geometry these are hemispheres with centers on the boundary of the equatorial disc. The dihedral angles of these planes are the angles of the polygon.

Consider two hyperbolic planes close to the equatorial plane, one slightly above and one slightly beneath, both perpendicular to the z -axis. These will intersect the previous planes at angles slightly smaller than $\pi/2$. The region defined by these N planes makes a hyperbolic polyhedron realizing the cell structure of the prism. Note that our construction completes the proof of Proposition 1.6, for the special case $C = Pr_N$, $N \geq 5$.



Figure 2:

For $N > 7$ we will construct D_N by cutting it into two prisms each with $N - 1$ faces and the dihedral angles shown below.

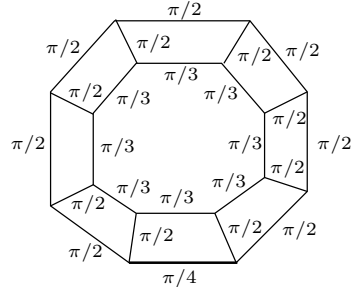
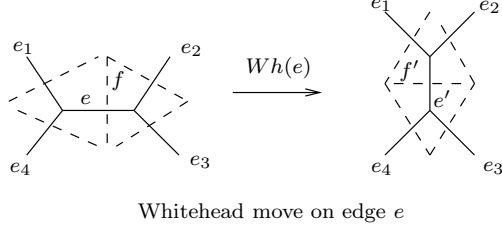


Figure 3:

These angles satisfy Andreev’s conditions (1) – (5) so we can use Newton’s method to deform the prism constructed in the previous paragraph to have these angles. Gluing this prism is to its mirror image, the edges labeled $\pi/2$ on the outside disappear as edges, and the edges labeled on the outside by $\pi/4$ glue together becoming an edge with dihedral angle $\pi/2$. Hence, we have constructed a polyhedron realizing D_N , assuming $N > 7$. Notice that when $N \leq 7$ the combinatorics of D_N coincides with that of Pr_N . \square

Assume that the two vertices incident at an edge e are trivalent. A Whitehead move $Wh(e)$ on edge e is given by the local change of the abstract polyhedron described in the following diagram. The Whitehead

move in the dual complex is dashed. Often we will find it convenient to describe the Whitehead move entirely in terms of the dual complex, in which case we write $Wh(f)$.



Whitehead move on edge e

Figure 4:

The following lemma appears in [25]:

Lemma 2.4 *Let the abstract polyhedron C' be obtained from the simple abstract polyhedron C by a Whitehead move $Wh(e)$. Then if \mathcal{P}_C^0 is non-empty so is $\mathcal{P}_{C'}^0$.*

The proof constructs a sequence of polyhedra realizing C with dihedral angles chosen so that the edge e converges to a single point at infinity. A carefully chosen small perturbation of this limiting configuration results in a compact polyhedron realizing C' with non-obtuse dihedral angles.

Suppose that we have a polyhedron realizing C with all dihedral angles equal to $\frac{2\pi}{5}$, and choose a small $\epsilon > 0$. To implement a Whitehead move using the computer, we assign dihedral angle ϵ to the edge e and dihedral angle $\frac{\pi}{2}$ to the four edges sharing an endpoint with e . Leaving the dihedral angles of the remaining edges the same, the resulting set of angles is in A_C and hence we can use Newton's Method to deform P into a polyhedron P_1 realizing C with these new angles.

If ϵ was chosen small enough, P_1 will be in the basin of attraction for a polyhedron realizing C' with the edge e' replacing e , the dihedral angle at e' equal to ϵ , and all other dihedral angles as in P_1 . We call the resulting polyhedron P_2 . Since C' is simple we can deform P_2 to have all dihedral angles $\frac{2\pi}{5}$, obtaining P' .

The following diagram shows these four steps when doing a Whitehead move on one of the edges of the dodecahedron. Here and elsewhere in this paper we use ϵ approximately $\frac{\pi}{45}$. (A smaller ϵ may be necessary when constructing polyhedra with a very large number of faces.)

If we can find a sequence of combinatorial Whitehead moves reducing a given simple abstract polyhedron C to either Pr_N or D_N via a sequence of simple abstract polyhedra C_1, \dots, C_N , we can use Newton's method to perform this sequence of Whitehead moves in the reverse order, constructing geometric polyhedra that realize C_N, C_{N-1}, \dots, C_1 , and finally C . Before explaining why such a sequence always exists, we demonstrate this process for the dodecahedron.

We can then use Newton's Method to do the reverse sequence of Whitehead moves $Wh(8, 11)$, $Wh(4, 11)$, $Wh(1, 2)$, $Wh(9, 11)$, $Wh(2, 4)$, $Wh(1, 6)$, $Wh(7, 11)$, $Wh(6, 9)$, $Wh(1, 5)$, and $Wh(1, 4)$ geometrically, constructing the dodecahedron from D_{12} . The following diagram shows this process.

2.6 A Lemma on Whitehead Moves

The following lemma from [8] and [25] is necessary to prove Andreev's Theorem and for our construction of simple polyhedra doing Whitehead moves geometrically with Newton's Method.

Lemma 2.5 Whitehead Sequence

Let C be a simple abstract polyhedron on \mathbb{S}^2 which is not a prism. If C has $N > 7$ faces, C can be simplified to D_N by a finite sequence of Whitehead moves such that all of the intermediate abstract polyhedra are simple.

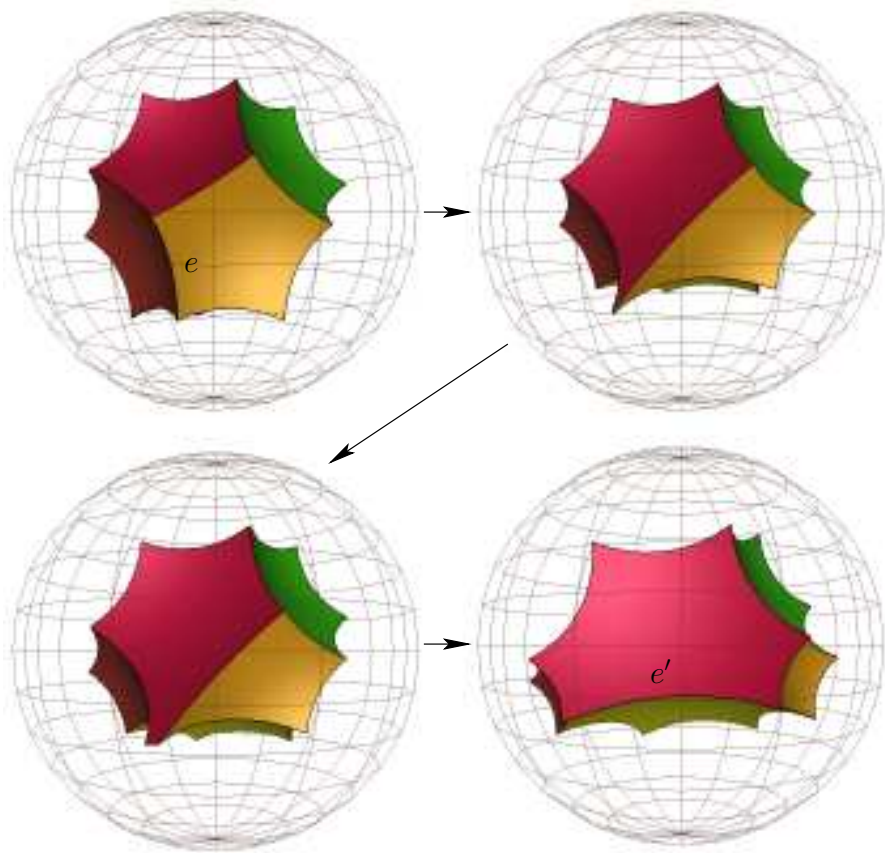


Figure 5: Whitehead move $Wh(e)$ on edge e of the dodecahedron

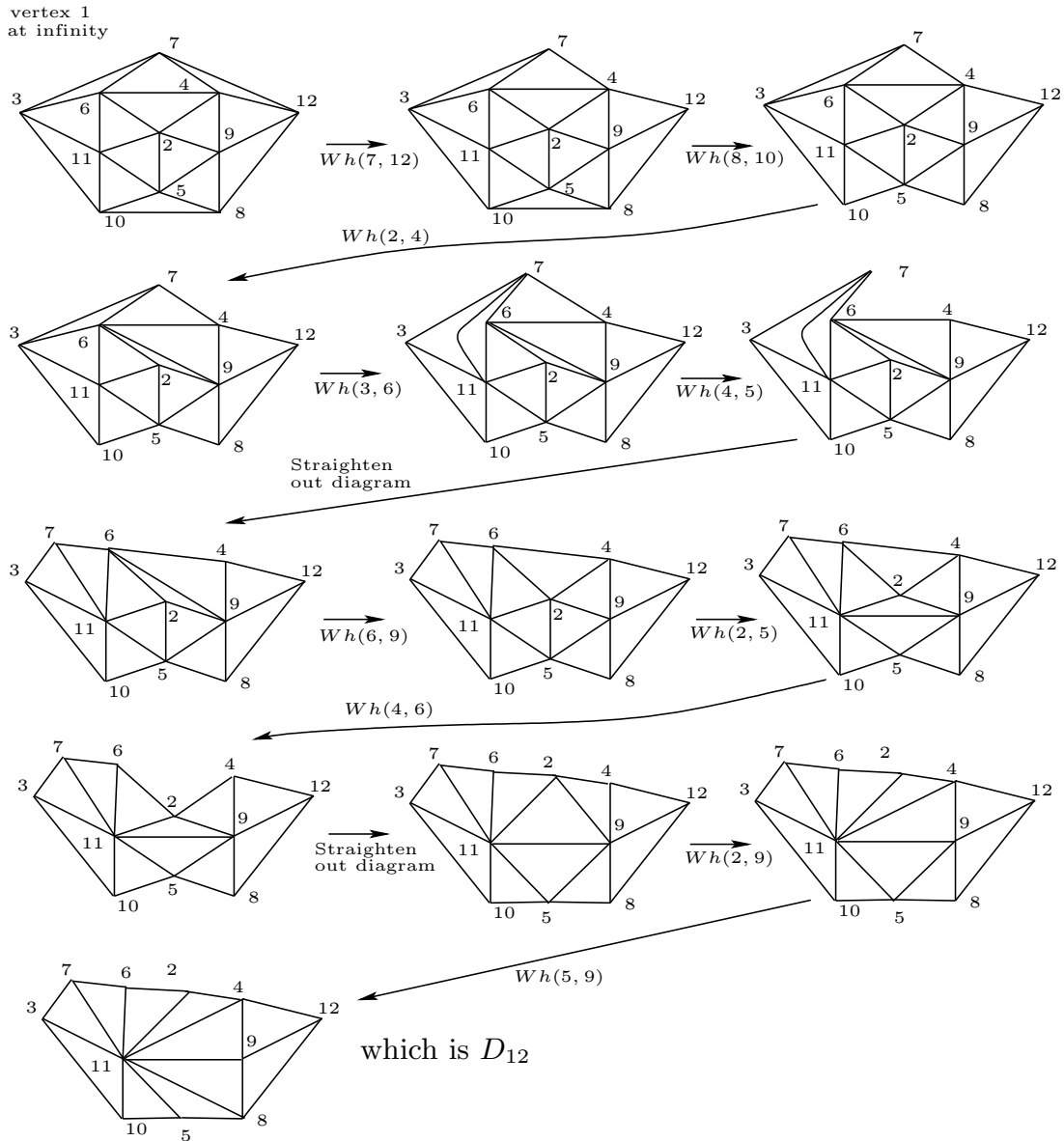


Figure 6:

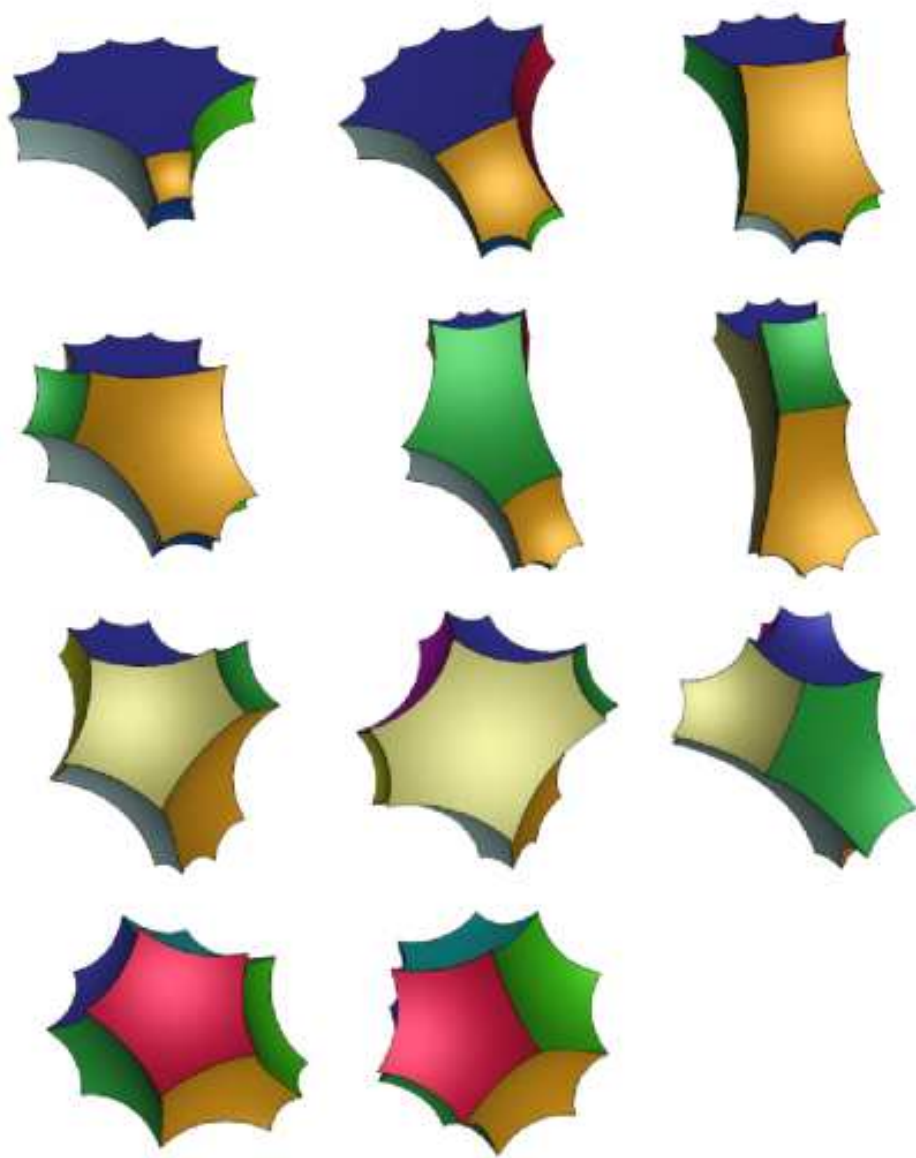


Figure 7: Construction of the dodecahedron from D_{12} using 10 Whitehead Moves.

Theorem 6 in Andreev's original paper contains our Lemma 2.5. Andreev's original proof of Theorem 6 provides an algorithm to produce the Whitehead moves needed for this lemma, but the algorithm *contains a glitch*. An error was detected when the author tried to implement it as a computer program. The algorithm failed on the first test, when given a dodecahedron.

In the instead using $Wh(6, 9)$ for the fifth Whitehead move of the sequence described in the previous section, Andreev's algorithm uses either $Wh(2, 6)$ or $Wh(2, 5)$. In both cases it produces an abstract polyhedron which had a prismatic 3-circuit, see below:

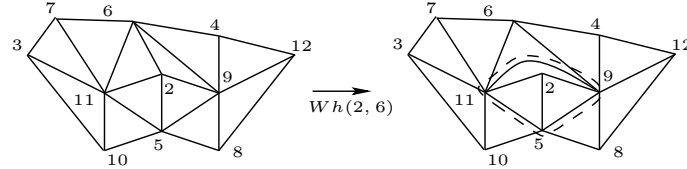


Figure 8:

In combination with the computer-implemented Whitehead move described in the previous section, the sequence of Whitehead moves given in the proof of Lemma 2.5 gives us the path that we will use for our homotopy method when constructing simple polyhedra. We provide an outline of the proof here that is sufficient to describe the sequence of Whitehead moves. Those who wish to see a complete proof may refer to [25, 41].

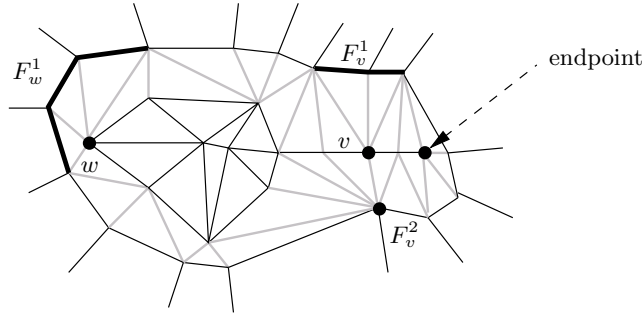
Outline of the Proof of Lemma 2.5:

We assume that $C \neq Pr_N$ is a simple abstract polyhedron with $N > 7$ faces. We will construct a sequence of Whitehead moves that change C to D_N , so that no intermediate complex has a prismatic 3-circuit.

Find a vertex v_∞ of C^* which is connected to the greatest number of other vertices. We will call the link of v_∞ , a cycle of k vertices and k edges, the *outer-polygon*. Most of the work is to show that we can do Whitehead moves to increase k to $N - 3$ without introducing any prismatic 3-circuits during the process. Once this is completed, it is easy to change the resulting complex to D_N^* by additional Whitehead moves.

Let us set up some notation. Draw the dual complex C^* in the plane with the vertex v_∞ at infinity, and the outer polygon P surrounding the remaining vertices and triangles. We call the vertices inside of P *interior vertices*. All of the edges inside of P which do not have an endpoint on P are called *interior edges*.

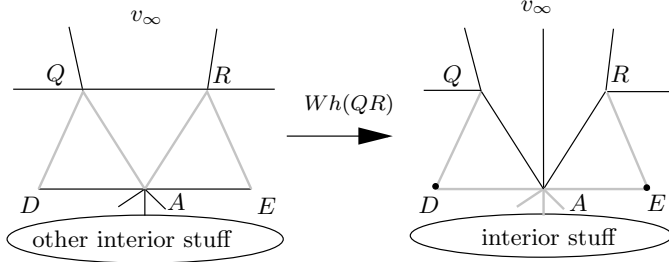
Note that the graph of interior vertices and edges is connected, since C^* is simple. An interior vertex which is connected to only one other interior vertex will be called an *endpoint*.



Throughout this proof we will draw P and the interior edges and vertices of C^* in black. The connections between P and the interior vertices will be grey. Connections between P and v_∞ will be black, if shown at all.

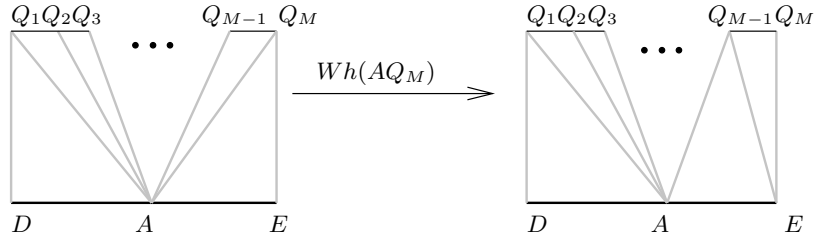
The link of an interior vertex v intersects P in a number of components F_v^1, \dots, F_v^n (possibly $n = 0$.) See the above figure. We say that v is *connected to P in these components*. Notice that since C^* is simple, an endpoint is always connected to P in exactly one such component.

Move 1 Suppose that there is an interior vertex A of C^* which is connected to P in exactly one component consisting of exactly two consecutive vertices Q and R . The Whitehead move $Wh(QR)$ on C^* increases the length of the outer polygon by one, and introduces no prismatic 3-circuit.

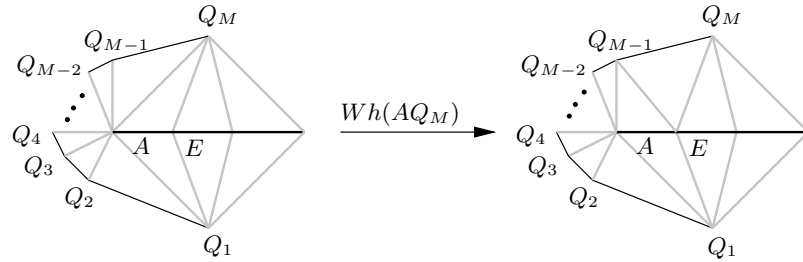


Move 2 Suppose that there is an interior vertex A that is connected to P in a component consisting of M consecutive vertices Q_1, \dots, Q_M of P (and possibly other components).

(a) If A is not an endpoint and $M > 2$, the sequence of Whitehead moves $Wh(AQ_M), \dots, Wh(AQ_3)$ results in a complex in which A is connected to the same component of P in only Q_1 and Q_2 . These moves leave P unchanged, and introduce no prismatic 3-circuit.

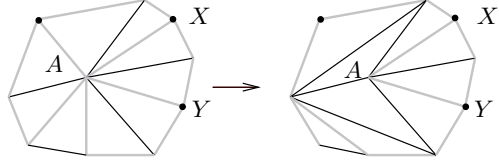


(b) If A is an endpoint and $M > 3$, the sequence of Whitehead moves $Wh(AQ_M), \dots, Wh(AQ_4)$ results in a complex in which A is connected to the same component of P in only Q_1, Q_2 , and Q_3 . These moves leave P unchanged and introduce no prismatic 3-circuits.



Note: In both parts (1) and (2), each of the Whitehead moves $Wh(AQ_M)$ transfers the connection between A and Q_M to a connection between the neighboring interior vertex E and Q_{M-1} . This is helpful in case 2 later.

Move 3 Suppose that there is an interior vertex A whose link contains two distinct vertices X and Y of P . Then there are Whitehead moves which eliminate any component in which A is connected to P , if that component does not contain X or Y . P is unchanged, and no prismatic 3-circuits will be introduced.



Here A is connected to P in four components containing six vertices. We can eliminate connections of A to all of the components except for the single-point components X and Y .

The proof that this move does not introduce any new prismatic 3-circuit is rather technical and depends essentially on the fact that A is connected to P in at least two other vertices X and Y . Andreev describes a nearly identical process to move 3 in his paper [8] on pages 333-334. However, he merely assumes that A is connected to P in at least one component in addition to the components being eliminated. He does not require that A is connected to P in at least *two vertices* outside of the components being eliminated. Andreev then asserts: “It is readily seen that all of the polyhedra obtained in this way are simple...” In fact, the Whitehead move demonstrated in Figure 2.6 creates a prismatic 3-circuit.

Having assumed this stronger (and incorrect) version of move 3, the remainder of Andreev’s proof is relatively easy. Unfortunately, the situation pictured in Figure 2.6 is not uncommon (as we will see in Case 3 below!) Restricted to the weaker hypotheses of Move 3 we will have to work a little bit harder.

Using Move 1, Move 2, and Move 3 we check that if the length of P is less than $N - 3$, then there is a sequence of Whitehead moves that increases the length of P by one without introducing any prismatic 3-circuits.

Case 1: An interior vertex that is not an endpoint connects to P in a component with two or more vertices, and possibly in other components.

Apply Move 2 decreasing this component to two vertices. We can then apply Move 3, eliminating any other components since this component contains two vertices. Finally, apply Move 1 to increase the length of the outer polygon by 1.

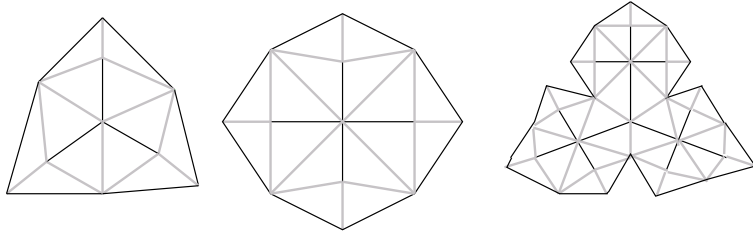
Case 2: An interior vertex that is an endpoint is connected to more than three vertices of P .

We assume that each of the interior vertices that are not endpoints are connected to P in components consisting of single vertices, otherwise we are in Case 1.

Let A be the endpoint which is connected to more than three vertices of P . By Move 2, part (2), there is a Whitehead move that transfers one of these connections to the interior vertex E that is next to A . Now, one of the components in which E is connected to P has exactly two vertices. The vertex E is not an endpoint since $k < N - 3$ implies that there are at least three interior vertices. Once this is done, we can apply Case 1.

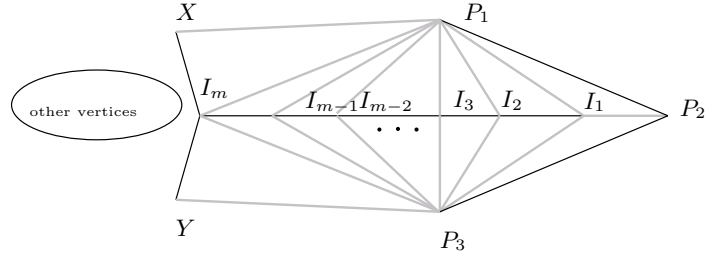
Case 3: Each interior vertex that is an endpoint is connected to exactly three vertices of P and each interior vertex which is not an endpoint is connected to P in components each consisting of a single vertex.

First, notice that if the interior vertices and edges form a line, the restriction on how interior vertices are connected to P results in the prism, contrary to the assumption that C is not the prism. However, there are many complexes satisfying the hypotheses of this case which have interior vertices and edges forming a graph more complicated than a line:



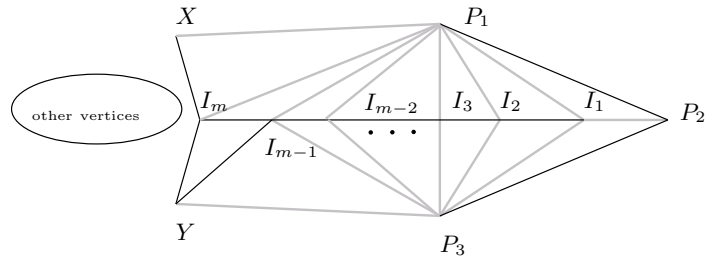
For such complexes we need a very special sequence of Whitehead moves to increase the length of P .

Pick an interior vertex which is an endpoint and label it I_1 . Denote by P_1 , P_2 , and P_3 the three vertices of P to which I_1 connects. I_1 will be connected to a sequence of interior vertices $I_2, I_3, \dots, I_m, m \geq 2$, with I_m the first interior vertex in the sequence that is connected to more than two other interior vertices. Vertex I_m must exist by the assumption that the interior vertices don't form a line segment, the configuration that we ruled out above. By hypothesis, I_2, \dots, I_m can only connect to P in components which each consist of a vertex, hence each must be connected to P_1 and to P_3 . Similarly, there is an interior vertex (call it X) which connects both to I_m and to P_1 and another vertex Y which connects to I_m and P_3 . Vertex I_m may connect to other vertices of P and other interior vertices, as shown on the left side of the following diagram.

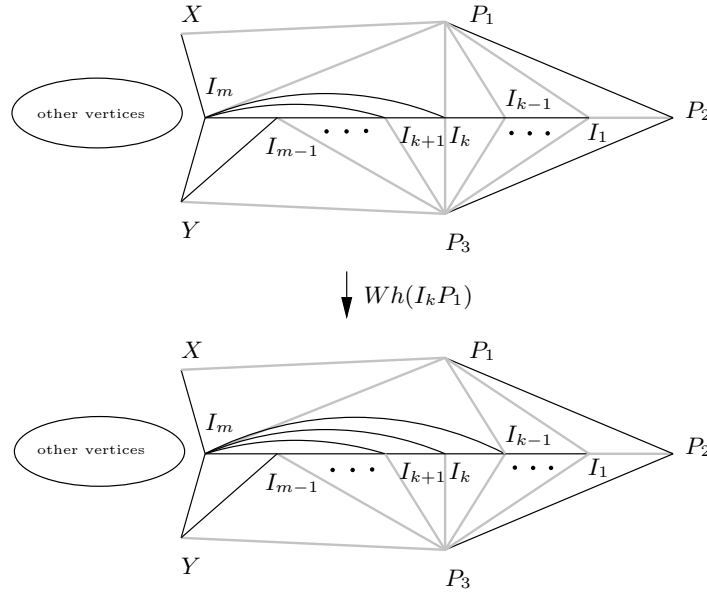


Now we describe a sequence of Whitehead moves that can be used to connect I_m to P in only P_1 and P_2 . This will allow us to use Move 1 to increase the length of P by one.

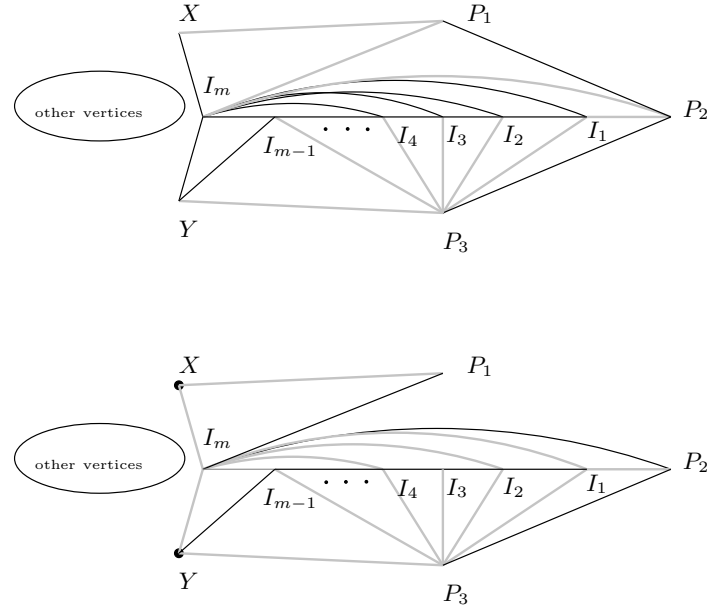
First, using Move 3 we can eliminate all possible connections of I_m to P in places other than P_1 and P_3 . Next, we do the move $Wh(I_mP_3)$ so that I_m connects to P only in P_1 .



Next, we must do the moves $Wh(I_{m-1}P_1), \dots, Wh(I_1P_1)$, in that order (see the figure below.)

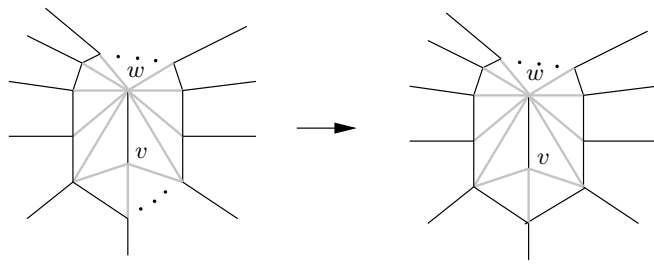


After this sequence of Whitehead moves we obtain the first diagram below, with I_m connected to P exactly at P_1 and P_2 , so that we can apply Move 1 to increase the length of P by the move $Wh(P_1P_2)$, below.



This concludes Case 3.

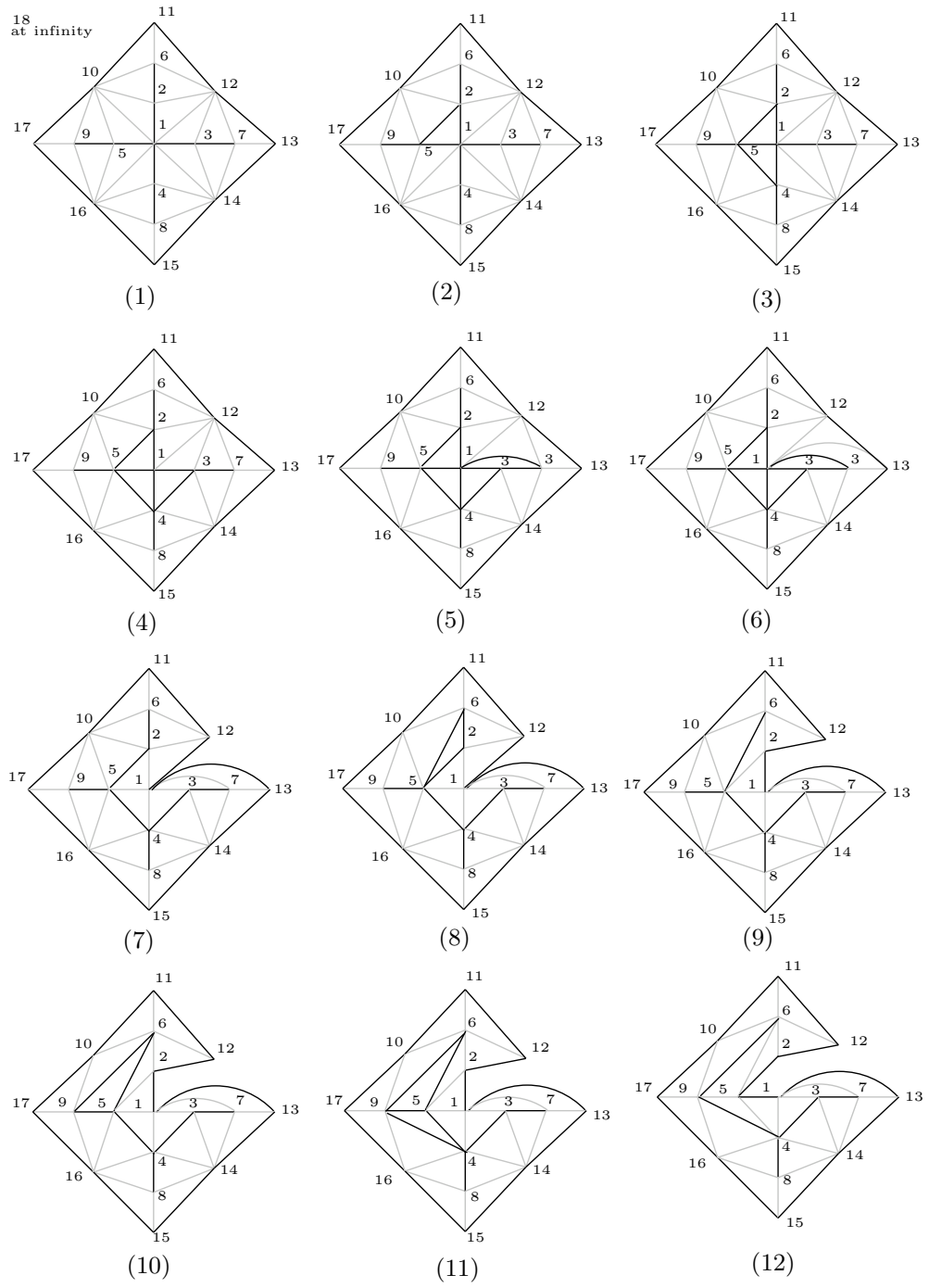
Since C^* must belong to one of these cases, we have seen that if the length of P is less than $N - 3$, we can do Whitehead moves to increase it to $N - 3$ without creating prismatic 3-circuits. Hence we can reduce to the case of two interior vertices, both of which must be endpoints. Then we can apply Move 2 part (b) to decrease the number of connections between one of these two interior vertices and P to exactly 3. The result is the complex D_N , as shown to the right below.



□

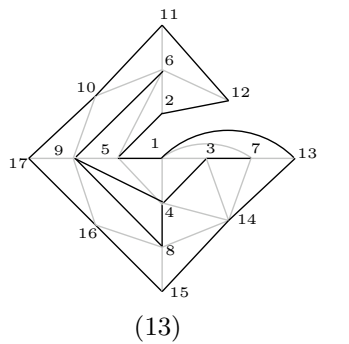
2.7 Construction of a “difficult” simple polyhedron

We illustrate the algorithm described in the previous section by constructing a hyperbolic polyhedron realizing an abstract polyhedron for which Case 3 from the proof of Lemma 2.5 is necessary, and hence is particularly difficult.

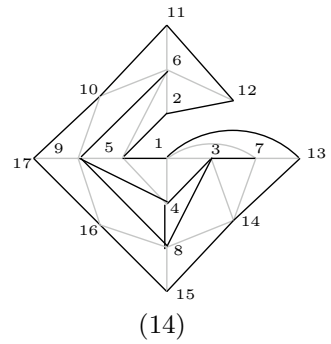


Case 3 from the proof of Lemma 2.5 is done in sub-figures (1)–(7).

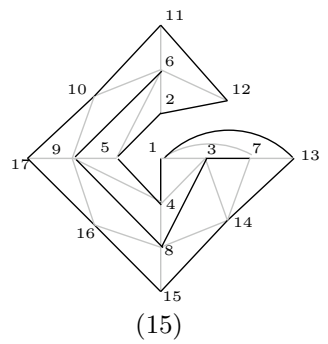
Case 1 follows in sub-figures (7)–(9) and again (for a different edge of P) in sub-figures (9)–(12).



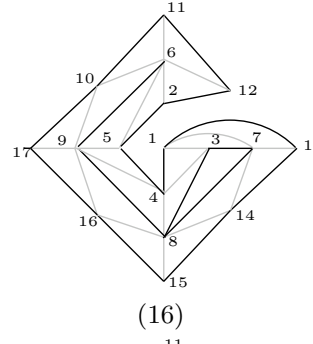
(13)



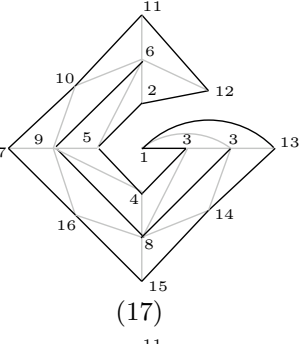
(14)



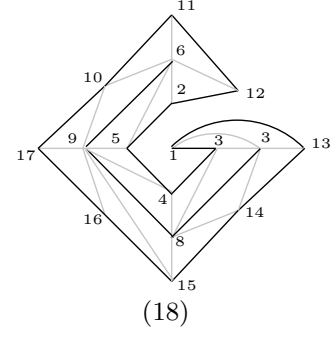
(15)



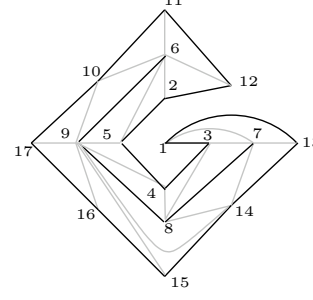
(16)



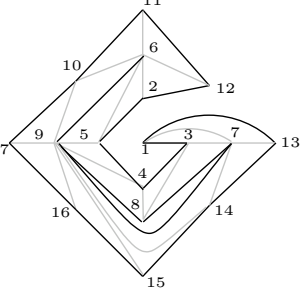
(17)



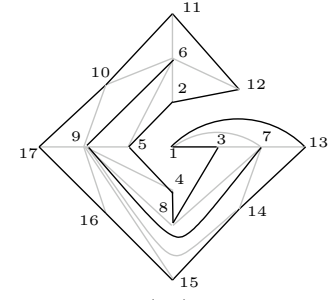
(18)



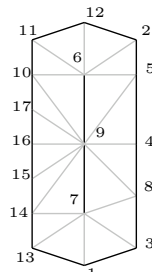
(19)



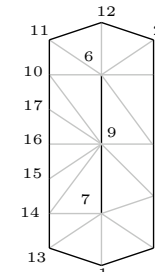
(20)



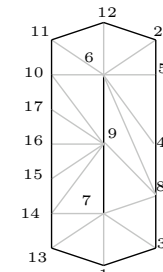
(21)



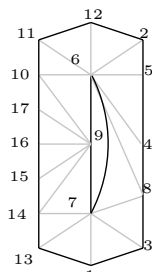
(22)



(23)

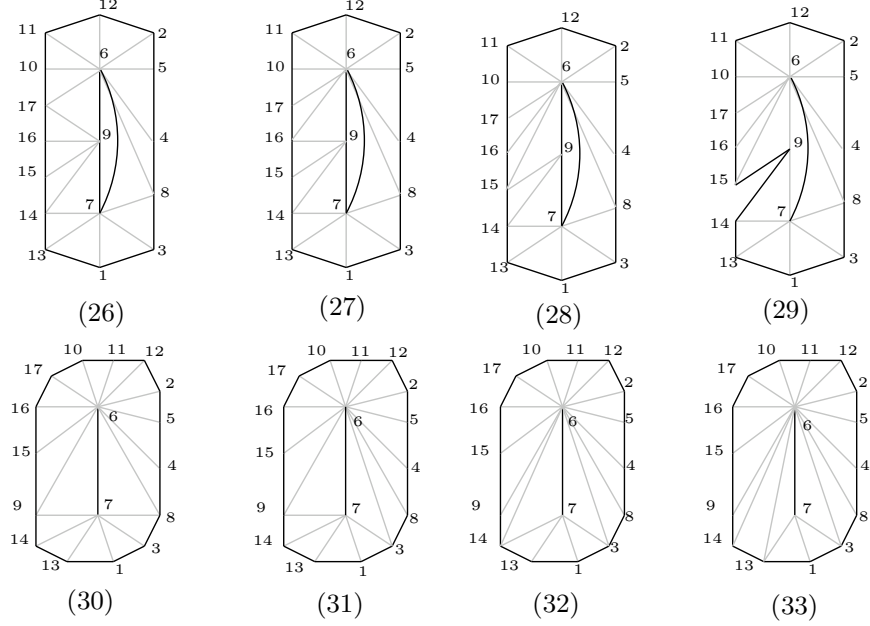


(24)



(25)

Case 1 is repeated three times in sub-figures (12)–(15), then (15)–(17), and finally in (17)–(21). The figure is straightened out between figures (21) and (22), then Case 1 is done in (22)–(29).



Continuing from the last page, sub-figures (22)–(29) are another instance of Case 1. The figure has been straightened out between sub-figures (29) and (30). A sequence of final Whitehead moves is done in sub-figures (30)–(33) so that one of the two interior vertices is only connected to three points on the outer polygon. This reduces the complex to D_{18}^* .

Following the Whitehead moves backwards from D_{18}^* back to R_{18}^* we find the following sequence of Whitehead moves.

$Wh(6, 13)$, $Wh(6, 9)$, $Wh(3, 6)$, $Wh(9, 12)$, $Wh(6, 15)$, $Wh(6, 16)$, $Wh(6, 17)$, $Wh(6, 7)$, $Wh(6, 8)$, $Wh(6, 4)$, $Wh(8, 18)$, $Wh(7, 9)$, $Wh(9, 14)$, $Wh(9, 15)$, $Wh(3, 18)$, $Wh(7, 8)$, $Wh(4, 18)$, $Wh(3, 8)$, $Wh(8, 9)$, $Wh(5, 18)$, $Wh(4, 9)$, $Wh(6, 9)$, $Wh(2, 18)$, $Wh(5, 6)$, $Wh(1, 18)$, $Wh(1, 13)$, $Wh(1, 3)$, $Wh(3, 4)$, $Wh(4, 5)$, $Wh(2, 5)$.

We did this sequence of Whitehead moves geometrically, using Newton's Method. The result, starting with D_{18} , and realizing R_{18} is shown in Figure 2.7. Each polyhedron is displayed in the conformal ball model.

2.8 Truncation of vertices

We have seen an outline of how to construct simple polyhedra. We now show how to construct all truncated polyhedra, except for the triangular prism, which we have already constructed in Section 2.5.

Lemma 2.6 *If $A_C \neq \emptyset$, then there are points in A_C arbitrarily close to $(\pi/3, \pi/3, \dots, \pi/3)$.*

Proof: Simply check that if $\mathbf{a} \in A_C$, then the entire straight line path to $(\pi/3, \pi/3, \dots, \pi/3)$, excluding the final point is in A_C . \square

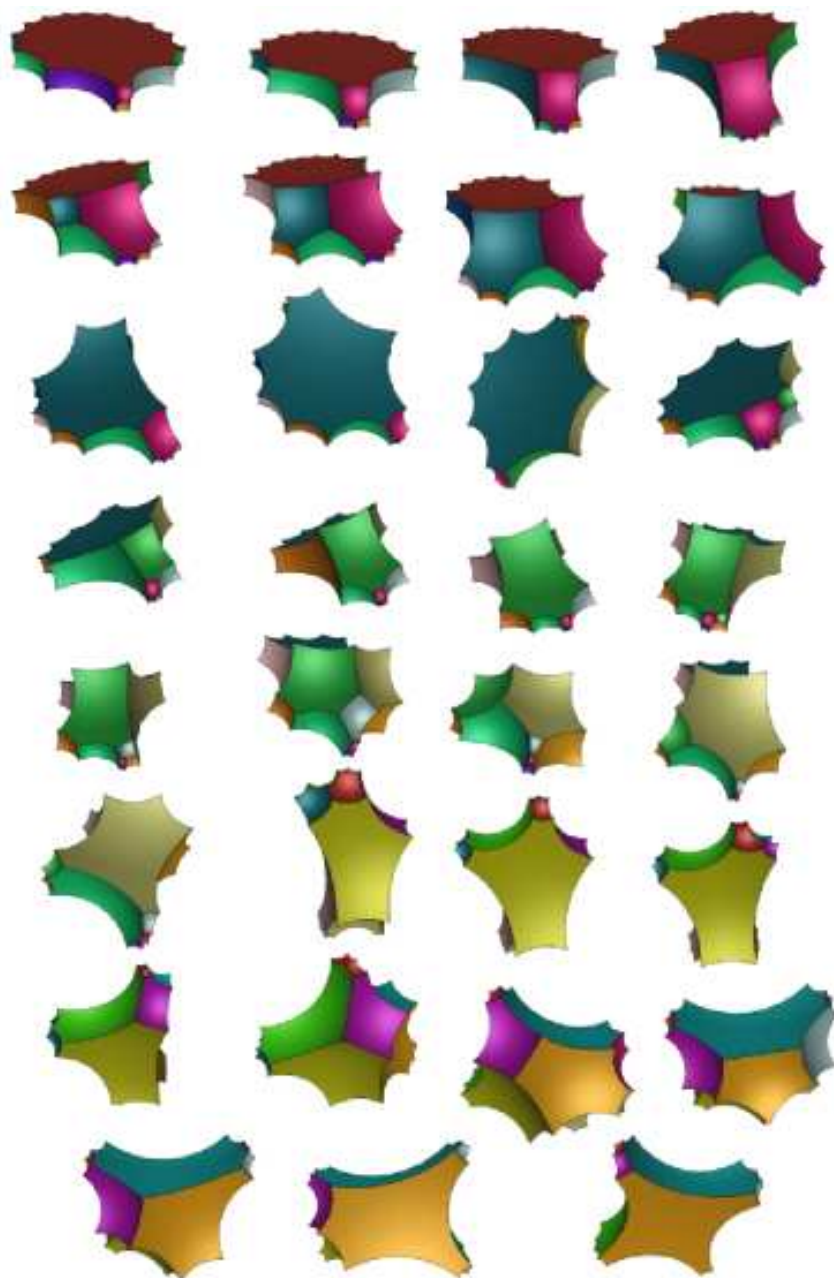


Figure 9: Construction of R_{18} from D_{18} using 30 Whitehead moves.

Thus we can assume that \mathbf{a} is arbitrarily close to $(\pi/3, \pi/3, \dots, \pi/3)$, because once we have a polyhedron realizing C with non-obtuse dihedral angles, we can deform it to have any dihedral angles in A_C , as described in Section 2.4. Specifically, choose some $0 < \delta < \frac{\pi}{18}$ and assume that each component of \mathbf{a} is within δ of $\frac{\pi}{3}$.

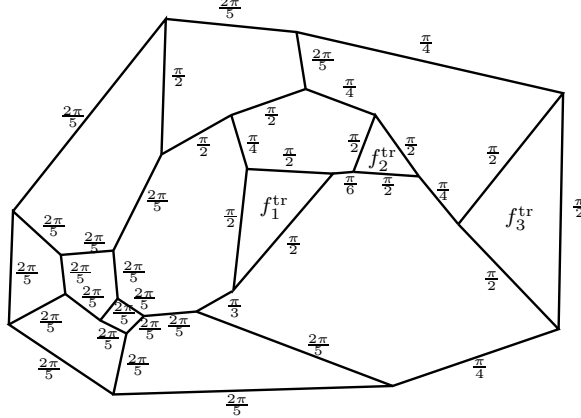
Let \tilde{C} be the C with each of the triangular faces f_i^{tr} replaced by a single vertex v_i^{tr} . (Or, if C is the truncated triangular prism, let \tilde{C} be the prism.) Let $\hat{\mathbf{a}}$ be the angles from \mathbf{a} corresponding to the edges from C that are in \tilde{C} and let $\beta = (\hat{\mathbf{a}}_1 + 2\delta, \hat{\mathbf{a}}_2 + 2\delta, \dots)$. (If \tilde{C} is the prism, re-number the edges so that the three edges forming the prismatic cycle are the first three, and choose $\beta = (\hat{\mathbf{a}}_1, \hat{\mathbf{a}}_2, \hat{\mathbf{a}}_1, \hat{\mathbf{a}}_5 + 2\delta, \hat{\mathbf{a}}_5 + 2\delta, \dots)$.)

Note that δ was chosen so that $\beta \in A_{\tilde{C}}$. Then, the straight line path $\mathbf{a}(t)$ joining β to $\hat{\mathbf{a}}$ (parameterized by $t \in (0, 1)$) will remain in $A_{\tilde{C}}$ except that the sum of the dihedral angles of edges meeting at each of the vertices v_i^{tr} will decrease past π at some time $t_i \in (0, 1)$.

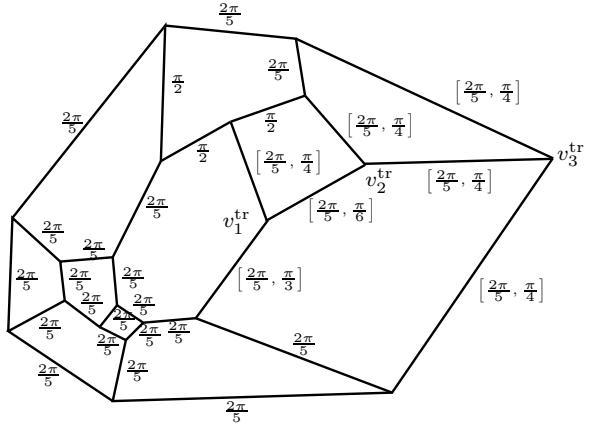
In [25, 41] the authors use the path $\mathbf{a}(t)$ to construct a sequence of polyhedra $\tilde{P} = P_0, P_1, \dots, P_{N-1} = P$ where \tilde{P} realizes C , and P_i is obtained from P_{i-1} truncating the vertices that become ideal when $t = t_i$. (The truncation is done using a small perturbation.) Realizing P proves that $\mathcal{P}_C^0 \neq \emptyset$, as needed for the proof of Andreev's Theorem.

Because the proof from [25, 41] gives us a priori knowledge that compact polyhedra exist realizing each of the intermediate combinatorial structures exist, we can use Newton's method to deform the planes forming \tilde{P} to realize the angles in the entire path $\mathbf{a}(t)$ without truncating each vertex once it meets $\partial_\infty \mathbb{H}^3$. We can then solve independently for the planes corresponding to the triangles in C so that each intersects the three appropriate planes at the three appropriate angles.

We illustrate this construction below for the following pair (C, \mathbf{a}) , which has three truncations labeled f_1^{tr} , f_2^{tr} , and f_3^{tr} .



The path $\mathbf{a}(t)$ described above works with any truncated C . For many C , such as the current one, a much easier path $\mathbf{a}(t)$ can be found satisfying conditions (1,3,4) and (5) from Andreev's Theorem for \tilde{C} , but for which the sum of the dihedral angles of the edges meeting at each v_i^{tr} decreases past π at some $t_i \in (0, 1)$. Such a path is sufficient for our construction. For the current construction, \tilde{C} is shown below with edges labeled according to an appropriate path $\mathbf{a}(t)$. (Notation: $\mathbf{a}(t) = \beta$ for the edges labeled with a single angle β , whereas $\mathbf{a}(t) = \eta(1-t) + \gamma t$ for the edges $[\eta, \gamma]$.)



We constructed a polyhedron \tilde{P} realizing the pair $(\tilde{C}, \mathbf{a}(0))$ and used Newton's method to deform the faces so that the dihedral angles follow the path $\mathbf{a}(t)$. After obtaining a non-compact polyhedron \tilde{P}_1 realizing angles $\mathbf{a}(1)$ we truncated the vertices $v_1^{tr}, v_2^{tr}, v_3^{tr}$. The final result is the polyhedron:



which will be used in the next section to form part of a compound polyhedron.

2.9 Constructing compound polyhedra

Any compound polyhedron can be constructed by gluing together a finite number of truncated polyhedra. We illustrate this construction for the polyhedron shown in Section 1.2.

In general, one cuts along every prismatic 3-circuit which does not correspond to a triangular face. Here there is one such circuit which is labeled γ . We cut along γ obtaining two combinatorial polyhedra for which every prismatic 3-circuit corresponds to a triangular face:

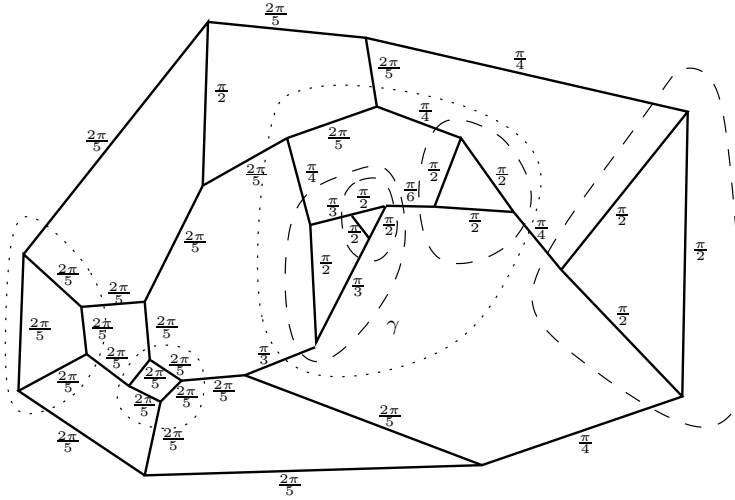
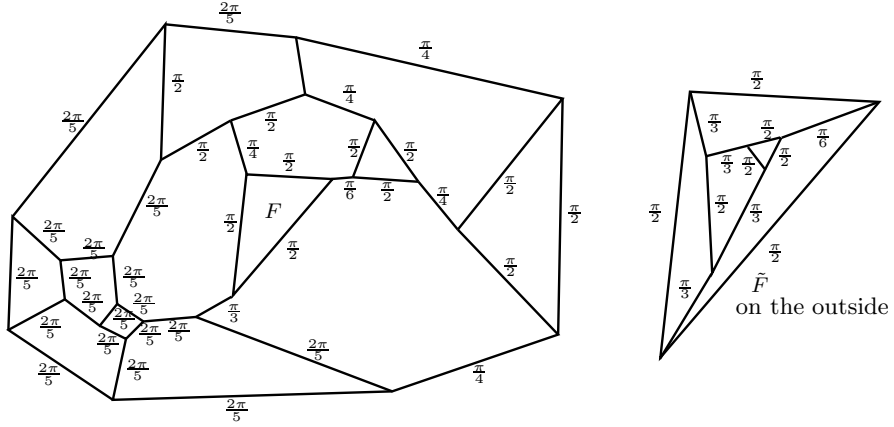
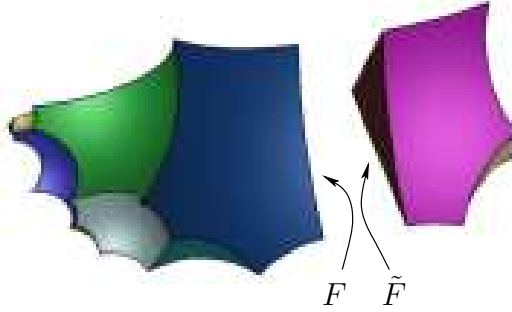


Figure 10:

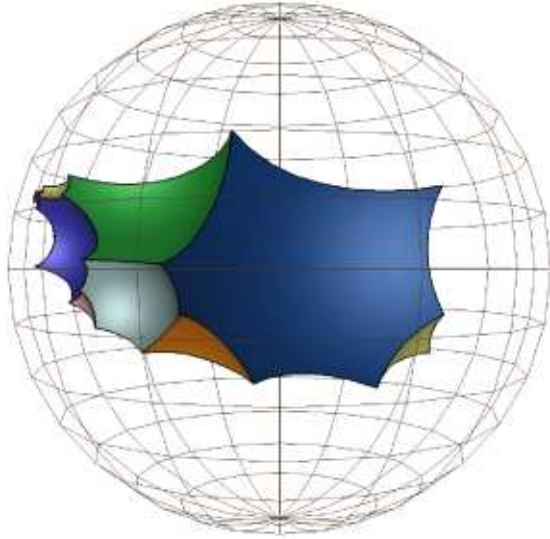


In this case, the diagram on the left is that for the polyhedron that we constructed in the previous section. The diagram on the right is that of the truncated triangular prism, which can also be easily constructed.

We require that the new triangular faces F and \tilde{F} obtained by cutting along γ be perpendicular to each of the other faces that they intersect. Then each face angle equals the dihedral angle outside of F , or \tilde{F} , that leads to that vertex. Because we obtained the two diagrams by cutting the original diagram along γ , the dihedral angles on the edges leading to F and \tilde{F} are the same and we naturally obtain that F and \tilde{F} have the same face angles, but are mirror images of each other.



These two polyhedra glue perfectly together to form a polyhedron realizing (C, \mathbf{a}) as shown in the following figure.



3 Applications to discrete groups and polyhedral orbifolds

Let P be a finite volume hyperbolic polyhedron having dihedral angles each of which is a proper integer sub-multiple of π . It is a well-known application of the Poincaré Polyhedron Theorem [20] that the group generated by reflections in the faces P forms a discrete subgroup Γ_P of $\text{Isom}(\mathbb{H}^3)$. Such groups have been extensively studied, see [55], and the references therein.

Given such a discrete reflection group Γ_P , we denote the corresponding orbifold by $O_P = \mathbb{H}^3/\Gamma_P$. We will use the term *polyhedral orbifolds* to describe orbifolds obtained in this way. (Note: often in the literature, the term “polyhedral orbifold” is used to describe the oriented double cover \mathbb{H}^3/Γ_P^+ , where Γ_P^+ is index two subgroup consisting of orientation preserving elements of Γ_P .) See Thurston [51, Chapter 13] and Reni [36] for more details on polyhedral orbifolds.

We use the computer program described in this paper to construct examples from three classes of polyhedral orbifolds, the Lambert cubes [28], the Löbell orbifolds [29, 52, 35], and an mysterious orbifold described by Mednykh and Vesnin [35] whose 16-fold cover is a “hyperelliptic” compact hyperbolic manifold.

We output the generators each reflection group as elements of $SO(3, 1)$ into SnapPea [58], computing volumes and length spectra of these orbifolds. For details on how SnapPea calculates the length spectrum refer to [22].

3.1 Construction of Lambert Cubes

A Lambert cube is a compact polyhedron realizing the combinatorial type of a cube, with three non-coplanar edges chosen and assigned dihedral angles α , β , and γ , and the remaining edges assigned dihedral angles $\frac{\pi}{2}$. It is easy to verify that if $0 < \alpha, \beta, \gamma < \frac{\pi}{2}$ then, such an assignment of dihedral angles satisfies the hypotheses of Andreev's Theorem. The resulting polyhedron is called the (α, β, γ) Lambert Cube, which we will denote by $P_{\alpha, \beta, \gamma}$. Thus, there are discrete reflection groups generated in the faces of a Lambert Cube when $\alpha = \frac{\pi}{p}$, $\beta = \frac{\pi}{q}$, and $\gamma = \frac{\pi}{r}$ for integers $p, q, r > 2$. We denote the corresponding orbifold $O_{\text{Lambert}}(p, q, r)$. In the following table, we present volumes and the lengths of the shortest geodesics for a sampling of Lambert Cubes for small p, q , and r :

$O_{\text{Lambert}}(3, 3, 3)$	Computed Volume: 0.324423	Theoretical Volume: 0.3244234492
Short Geodesics	6 mI 1.087070 6 mI 1.400257 3 mI $1.601733 + i \cdot 2.765750$ 6 mI 1.864162 4 mI 2.174140	3 mI $1.087070 + i \cot 2\pi/3$ 6 mI $1.400257 + i \cdot \pi$ 3 mI $1.790480 + i \cdot 0.762413$ 3 mI 2.138622 6 mI $2.199243 + i \cdot 2.436822$
$O_{\text{Lambert}}(3, 4, 5)$	Computed Volume: 0.479079	Theoretical Volume: 0.4790790206
Short Geodesics	2 mI 0.622685 1 mI $0.622685 + i \cdot 2.513274$ 1 mI $0.883748 + i \cdot 1.570797$ 1 mI 1.123387 1 mI 1.245371	1 mI $0.622685 + i \cdot 1.256637$ 3 mI 0.883748 1 mI $0.883748 + i \cdot 3.141592$ 1 mI $1.123387 + i \cdot 3.141593$
$O_{\text{Lambert}}(4, 4, 4)$	Computed Volume: 0.554152	Theoretical Volume: 0.5382759501
Short Geodesics	2 mI 0.175240 1 mI $0.175240 + i \cdot 1.108797$ 1 mI $0.175240 + i \cdot 0.739198$ 1 mI $0.175240 + i \cdot 1.847996$ 1 mI $0.175240 + i \cdot 2.587194$ 1 mI 0.350479	1 mI $0.175240 + i \cdot 0.369599$ 1 mI $0.175240 + i \cdot 0.739198$ 1 mI $0.175240 + i \cdot 1.478396$ 1 mI $0.175240 + i \cdot 2.217595$ 1 mI $0.175240 + i \cdot 2.956793$
$O_{\text{Lambert}}(5, 8, 12)$	Computed Volume: 0.768801	Theoretical Volume: 0.7688005863
Short Geodesics	3 mI 0.407809 1 mI $0.407809 + i \cdot 1.047198$ 1 mI $0.407809 + i \cdot 2.094396$ 1 mI $0.407809 + i \cdot 3.141592$ 1 mI $0.643110 + i \cdot 0.785398$ 1 mI $0.643110 + i \cdot 2.356194$	1 mI $0.407809 + i \cdot 0.523599$ 1 mI $0.407809 + i \cdot 1.570797$ 1 mI $0.407809 + i \cdot 2.617995$ 2 mI 0.643110 1 mI $0.643110 + i \cdot 1.570796$ 1 mI $0.643110 + i \cdot 3.141593$

The format of the lists of Geodesic lengths presented in this and in the following tables, is the same as that presented by SnapPea. The first entry is the multiplicity of distinct geodesics having the same complex length. The second entry is either “mI” to indicate that the geodesic has the topological type of a mirrored interval or is empty, if the geodesic has the topological type of a circle. The third entry is the complex length. Nearly all of the short geodesics that we present in these tables are mirrored intervals because our orbifolds are mirrored polyhedra and because we have only listed rather short geodesics.

Also notice, that while SnapPea provides many more digits of precision for the geodesic length, we have rounded to the first 6 decimal places in order to group geodesics that are likely to correspond to the same class, but weren't listed that way due to numerical imprecision.

The volumes of Lambert cubes have been explicitly calculated by R. Kellerhals [28]. If we write $\Delta(\eta, \xi) = \Lambda(\eta + \xi) - \Lambda(\eta - \xi)$, where Λ is the well-known Lobachevskii function $\Lambda(x) = -\int_0^x \log |2 \sin(t)| dt$, then

$$\text{Vol}(P_{\alpha,\beta,\gamma}) = \frac{1}{4} \left(\Delta(\alpha, \theta) + \Delta(\beta, \theta) + \Delta(\gamma, \theta) - 2 \cdot \Delta\left(\frac{\pi}{2}, \theta\right) - \Delta(0, \theta) \right). \quad (3)$$

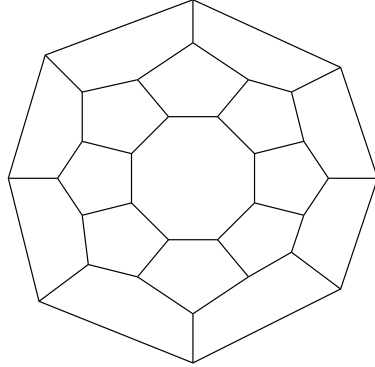
where θ , with $0 < \theta < \frac{\pi}{2}$ is the parameter defined by:

$$\begin{aligned} \tan^2(\theta) &= p + \sqrt{p^2 + L^2 M^2 N^2}, \\ p &= \frac{L^2 + M^2 + N^2 + 1}{2}, \text{ and} \\ L &= \tan\alpha, M = \tan\beta, N = \tan\gamma. \end{aligned}$$

The column in the above table labeled “approximate volume” gives the volume of $O_{\text{Lambert}}(p, q, r)$ as computed using SnapPea, while the column labeled “actual volume” gives the volume of $O_{\text{Lambert}}(p, q, r)$ computed using Equation 3.

3.2 Construction of Löbell Orbifolds

For each $n > 5$, there is an radially symmetric combinatorial polyhedron having two n -sided faces and having $2n$ faces with 5 sides which provides a natural generalization of the dodecahedron. This combinatorial polyhedron is depicted below for $n = 8$.



Andreev’s Theorem provides the existence of a compact right angled polyhedron R_n realizing this abstract polyhedron because it contains no prismatic 3-circuits or prismatic 4-circuits. (In fact, the work of Löbell predates Andreev by many years, and one can also verify the existence of R_n as an appropriate truncation and gluing of tetrahedra.) We refer to the group generated by reflections in the faces of R_n by Γ_n and the corresponding orbifold $O_{\text{Löbell}}(n) = \mathbb{H}^3/\Gamma_n$.

Historical Note:

While we restrict our attention to the orbifold $O_{\text{Löbell}}(n)$ in this paper, the reader may wish to notice that the first example of a closed hyperbolic manifolds was constructed by Löbell [29] in 1931 by an appropriate gluing of 8 copies of R_5 . Generalizing this notion, Vesnin [52] has described a convenient algebraic method to construct a torsion free subgroup $\Gamma'_n \subset \Gamma_n$ of index 8. This, in the n -th *Löbell Manifold* is the compact, orientable, hyperbolic manifold $M_{\text{Löbell}}(n) := \mathbb{H}^3/\Gamma'_n$. Naturally, $M_{\text{Löbell}}(n)$ is an 8-fold (orbifold) cover of $O_{\text{Löbell}}(n)$. We refer the reader to the nice exposition in [52, 35] for the details. The delightful paper by Reni [36] provides further details on the construction of hyperbolic manifolds and orbifolds and finite covers of right-angled polyhedra.

We include the following table of data computed using SnapPea for the $n = 5, \dots, 8$ Löbell orbifolds.

$O_{\text{Löbell}}(5)$ (Dodecahedron)	Computed Volume: 4.306208	Theoretical Volume: 4.3062076007
Short Geodesics	60 mI 2.122550 60 mI 2.938703 126 mI 3.233843 60 mI 3.783112 + $i \cdot 1.376928$ 12 3.835986 + $i \cdot \pi$ 60 mI 3.966774	60 mI 2.122550 + $i \cdot \pi$ 60 mI 2.938703 + $i \cdot \pi$ 60 mI 3.579641 12 3.835986 60 mI 3.835986 + $i \cdot \pi$ 60 mI 4.0270318 + $i \cdot 2.264758$
$O_{\text{Löbell}}(6)$	Computed Volume: 6.023046	Theoretical Volume: 6.0230460200
Short Geodesics	36 mI 1.762747 37 mI 2.292431 48 mI 2.633916 36 mI 2.887271 48 mI 3.088970 24 mI 3.256614	12 mI 1.762747 + $i \cdot \pi$ 12 mI 2.292431 + $i \cdot \pi$ 24 mI 2.633916 + $i \cdot \pi$ 24 mI 2.887271 + $i \cdot \pi$ 12 mI 3.154720 + $i \cdot 1.312496$ 36 mI 3.256614 + $i \cdot \pi$
$O_{\text{Löbell}}(7)$	Computed Volume: 7.563249	Theoretical Volume: 7.5632490914
Short Geodesics	42 mI 1.611051 1 mI 1.823106 14 mI 2.388409 + $i \cdot \pi$ 14 mI 2.512394 + $i \cdot \pi$ 70 mI 2.898149 42 mI 2.898149 + $i \cdot \pi$	14 mI 1.611051 + $i \cdot \pi$ 42 mI 2.388409 14 mI 2.512394 14 mI 2.601666 14 mI 2.898149 + $i \cdot 1.280529$ 14 mI 3.031090 + $i \cdot \pi$
$O_{\text{Löbell}}(8)$	Computed Volume: 9.019053	Theoretical Volume: 9.0190527274
Short Geodesics	49 mI 1.528571 80 mI 2.448452 16 mI 2.760884 + $i \cdot 1.261789$ 48 mI 2.914035 + $i \cdot \pi$ 32 mI 3.057142 + $i \cdot \pi$ 64 mI 3.553688	16 mI 1.528571 + $i \cdot \pi$ 32 mI 2.448452 + $i \cdot \pi$ 32 mI 2.914035 160 mI 3.057142 16 mI 3.461816 + $i \cdot 2.650944$ 32 mI 3.553688 + $i \cdot \pi$

The column labeled “Computed Volume” gives the volume as computed in SnapPea, whereas “Theoretical Volume” provides the volume of $O_{\text{Löbell}}(n)$ using explicit formula from [53]. (In fact we have divided by 8 the volume formula presented in [53], because they study the volume of the 8-fold cover $M_{\text{Löbell}}(n)$.) If we let $\theta = \frac{\pi}{2} - \arccos\left(\frac{1}{2\cos(\pi/n)}\right)$, then

$$\text{Vol}(O_{\text{Löbell}}(n)) = \frac{n}{2} \left(2\Lambda(\theta) + \Lambda\left(\theta + \frac{\pi}{n}\right) + \Lambda\left(\theta - \frac{\pi}{n}\right) - \Lambda\left(2\theta + \frac{\pi}{2}\right) \right). \quad (4)$$

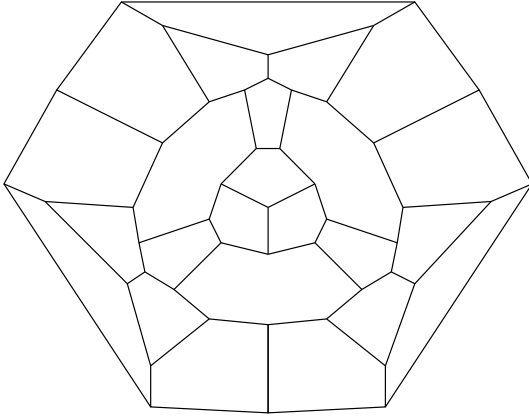
where Λ is the Lobachevskii function.

Notice that for each of the Löbell orbifolds that we computed, the volume computed in SnapPea agrees perfectly (within the six digits of precision available) with that given by Equation 4.

3.3 An orbifold due to Mednykh and Vesnin

In a very similar way to the construction of Löbell manifolds, Mednykh and Vesnin describe in [35] a compact three-dimensional hyperbolic manifold G which forms a 2-fold branched cover over the sphere \mathbb{S}^3 . They call manifolds with such a covering property over \mathbb{S}^3 “hyperelliptic,” generalizing the classical notion of hyperelliptic Riemann surfaces. See also [32, 34, 33].

The combinatorial polyhedron considered by Mednykh and Vesnin (and apparently originally due to Grinbergs) is depicted below.



This abstract polyhedron has no prismatic 3-circuits or prismatic 4-circuits, so Andreev's Theorem guarantees the existence of a polyhedron R_{MV} realizing it with $\pi/2$ dihedral angles. We denote the group generated by reflections in the faces of R_{MV} by Γ_{MV} and the orbifold by O_{MV} . Combinatorial details on the construction of M_{MV} as a 16-fold cover of O_{MV} can be found in [35].

The following table contains invariants of the orbifold $O_{MV} = \mathbb{H}^3/\Gamma_{MV}$ obtained by entering an explicit list of generators for Γ_{MV} into SnapPea.

O_{MV}	Computed Volume: 6.023046	Theoretical Volume: unknown
Short Geodesics	9 mI 0.989308	3 mI $0.989308 + i \cdot \pi$
	9 mI 1.183451	3 mI $1.183451 + i \cdot \pi$
	18 mI 1.834468	6 mI $1.834468 + i \cdot \pi$
	18 mI 1.859890	6 mI $1.859890 + i \cdot \pi$
	27 mI 1.882318	9 mI $1.882318 + i \cdot \pi$
	6 mI 1.978616	3 mI $1.978616 + i \cdot \pi$
	9 mI 2.214787	3 mI $2.214787 + i \cdot \pi$
	18 mI 2.252719	6 mI $2.252719 + i \cdot \pi$
	6 mI 2.366902	3 mI $2.366902 + i \cdot \pi$
	6 mI 2.433170	6 mI $2.433170 + i \cdot \pi$
	6 mI 2.446977	6 mI $2.446977 + i \cdot \pi$

As an application, we obtain the estimate $\text{Vol}(M_{MV}) = 16 \cdot 15.608119 = 249.729904$ using that M_{MV} is a 16-fold orbifold cover over O_{MV} .

3.4 Spectral Staircases

For a given hyperbolic manifold or orbifold M , the “spectral staircase” is a plot of the number of closed geodesics of length less than l , which we denote $N(l)$, versus l . (In fact, it is much more common to plot $\log(N(l))$ due to the exponential growth predicted by (5) below.) The spectral staircase provides both a nice way to graphically display the spectrum of M and a illustration of the classical result of Margulis [31], who proves the following universal formula for the asymptotics of $N(l)$:

$$N(l) \sim \frac{\exp(\tau l)}{\tau l} \text{ as } l \rightarrow \infty \quad (5)$$

where the constant τ is the topological entropy, which for hyperbolic space \mathbb{H}^d is given by $\tau = d - 1$. For an exposition and nice experimental works considering spectral staircases, see [26] and the references within.

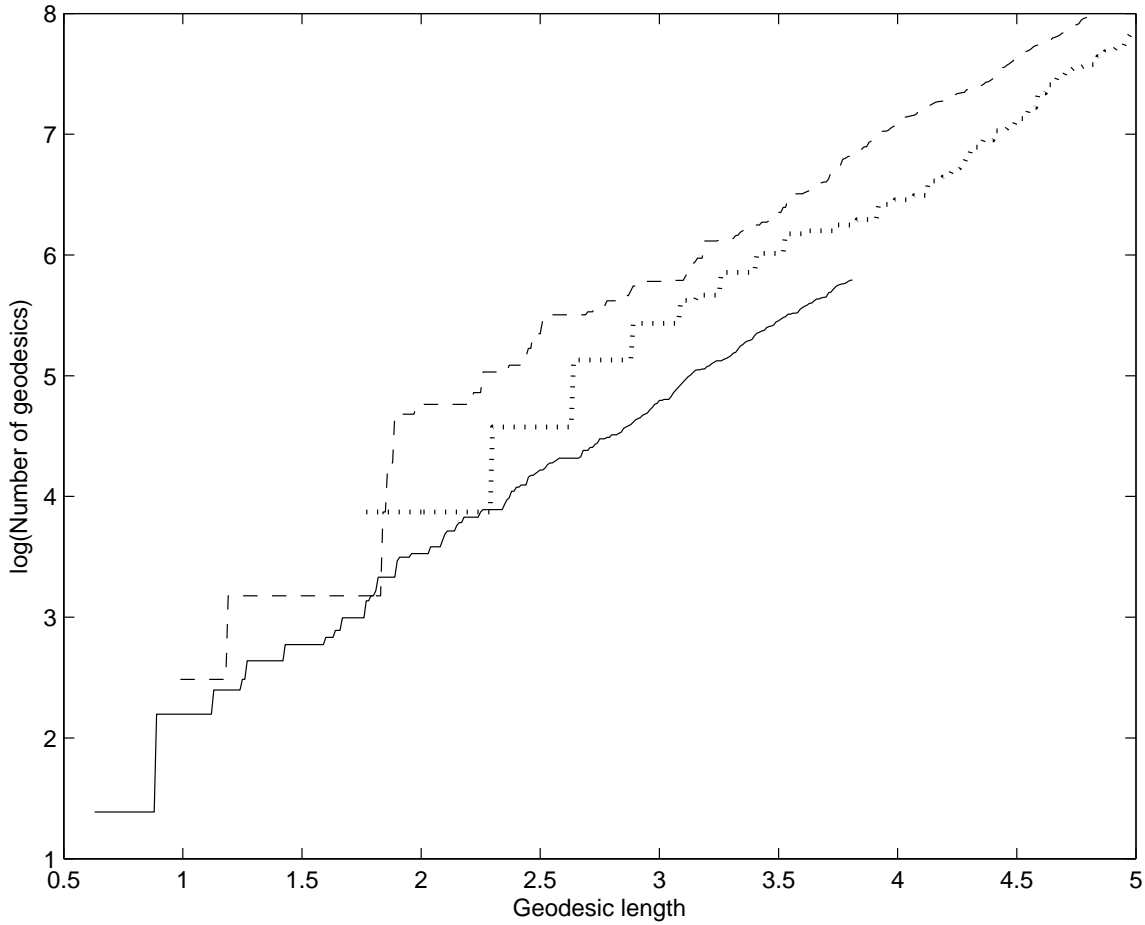


Figure 11: Spectral Staircases for the $O_{\text{Lambert}}(3, 4, 5)$ (solid line), $O_{\text{Löbell}}(6)$ (dotted line), and O_{MV} (dashed line).

We compute these spectral staircases for $O_{\text{Lambert}}(3, 4, 5)$, $O_{\text{Löbell}}(6)$, and O_{MV} displaying the results in Figure 3.4. (The data for $O_{\text{Lambert}}(3, 4, 5)$ ends at roughly $l = 3.8$. SnapPea encounters an error computing at this length, probably due to the comparatively small dihedral angles of $O_{\text{Lambert}}(3, 4, 5)$.)

4 Questions for further study

We present a non-comprehensive list of interesting questions for further study:

- 1 Determine if there is a faster way of computing Andreev Polyhedra.
- 1b Related question: determine if CirclePack [50] can be used to construct compact hyperbolic polyhedra and their reflection groups. If so, it would provide a faster method of construction.
- 2 Construct manifold covers of the polyhedral orbifolds that were considered in Section 3, including the Löbell Manifolds [52] the ‘‘Small Covers of the Dodecahedron’’ [17], and the Hyperelliptic Manifold [35]. Such a construction, could potentially lead to computations of many additional interesting invariants of these manifolds using SnapPea, as well as on drilling and Dehn fillings on them (which would also be possible in SnapPea).

- 2b Related question: use the program SNAP [18] to compute arithmetic invariants for these manifolds.
- 2c Related question: using SNAP, or the ideas used in SNAP [14], study the arithmetic invariants of polyhedral reflection groups.
- 3 Perform a study of volumes of hyperbolic polyhedra corresponding to general angles in A_C . (While SnapPea computes volumes only for polyhedra with discrete reflection groups, the functions from the SnapPea kernel could probably be used for this more general study.)

Appendix:

A Using the program to construct compact polyhedra and their reflection groups

The computer program described in this paper is a functional but slightly rough collection of Matlab [1] (or Octave [2]) scripts. Using a single command the program produces a polyhedron realizing a simple abstract polyhedron C with all dihedral angles $\frac{2\pi}{5}$. However, one must do a little bit more work to construct a polyhedron realizing (C, \mathbf{a}) of truncated or compound type. These later steps are not as automatic in the program, but one can follow the description in this paper step by step to do them “by hand.” Please see the README file enclosed with the program for further information.

There are two ways to output a polyhedron that has been constructed using this program: the *Object File Format* (e.g. “filename.off”) and the *Generators File Format* (e.g. “filename.txt”). The *Object File Format* output can be read into Geomview [3] and displayed nicely in the Poincaré Ball model there. The *Generators File Format* is for SnapPea [58] and (if the polyhedron output this way has dihedral angles that are proper integer sub-multiples of π) this file can be loaded into SnapPea.

An analysis of the computational complexity of this method would be quite involved and is not feasible at this point. In fact, the computational complexity of Newton’s Method is quite difficult [47, 46, 48, 49, 7].

In practice, on a contemporary PC running Linux, the most complicated construction in this paper took approximately 2 minutes; it is by no means fast, but certainly usable. We expect that the program described in this paper can be used to construct all polyhedra having no more than 30 faces and having dihedral angles bounded away from ∂A_C (with the exception of the part of ∂A_C corresponding to dihedral angles $\pi/2$, where there should be no problem.) Certainly the number of iteration steps in each homotopy (the parameter K from Section 2.4) and the parameter ϵ used in the Whitehead move (see Section 2.5) may need to be modified in special circumstances. With improvements of the program, perhaps by implementing it in a faster programming language, and, if necessary, in a higher precision arithmetic, we expect the same to be possible for up to 100 faces, or possibly more.

Acknowledgments:

The author gratefully thanks John H. Hubbard for suggesting that he write this program and for providing an outline for using the homotopy method in combination with Andreev’s proof. It was this suggestion that led to the discovery of the error in Andreev’s proof [25, 41] and eventually to a working program. The author has greatly benefited from many discussions with William D. Dunbar and he also thanks Rodrigo Perez and Travis Waddington for providing suggestions about the manuscript and attached computer files.

The computer program SnapPea, written by Jeff Weeks and his collaborators has allowed for the exciting applications in Section 3 of this paper. The author thanks Jeff Weeks and his collaborators for writing this wonderful program, and also thanks Jeff Weeks for helpful personal communications.

The author also gratefully thanks the referee who offered many suggestions which have led to a clearer explanation of why we use the technique that we use. His or her comments have also provided the inspiration for the last two sections of this paper, and significant further research in these directions.

References

- [1] www.mathworks.com.
- [2] www.octave.org.
- [3] www.geomview.org, Developed by The Geometry Center at the University of Minnesota in the late 1990's.
- [4] Colin Adams, Martin Hildebrand, and Jeffrey Weeks. Hyperbolic invariants of knots and links. *Trans. Amer. Math. Soc.*, 326(1):1–56, 1991.
- [5] D. V. Alekseevskij, È. B. Vinberg, and A. S. Solodovnikov. Geometry of spaces of constant curvature. In *Geometry, II*, volume 29 of *Encyclopaedia Math. Sci.*, pages 1–138. Springer, Berlin, 1993.
- [6] Eugene L. Allgower and Kurt Georg. *Numerical Continuation Methods, an introduction*. Springer-Verlag, 1990.
- [7] Carlos Beltrán Álvarez. Sobre el Problema 17 de Smale: Teoría de la intersección y geometría integral. Doctoral thesis (In Spanish), September 2006. Universidad de Cantabria.
- [8] E. M. Andreev. On convex polyhedra in Lobacevskii spaces (English Translation). *Math. USSR Sbornik*, 10:413–440, 1970.
- [9] E. M. Andreev. On convex polyhedra in Lobacevskii spaces (in Russian). *Mat. Sb.*, 81(123):445–478, 1970.
- [10] Xiliang Bao and Francis Bonahon. Hyperideal polyhedra in hyperbolic 3-space. *Bull. Soc. Math. France*, 130(3):457–491, 2002.
- [11] Lenore Blum, Felipe Cucker, Michael Shub, and Steve Smale. *Complexity and real computation*. Springer-Verlag, New York, 1998. With a foreword by Richard M. Karp.
- [12] Phil Bowers and Kenneth Stephenson. A branched Andreev-Thurston theorem for circle packings of the sphere. *Proc. London Math. Soc. (3)*, 73(1):185–215, 1996.
- [13] Bennett Chow and Feng Luo. Combinatorial Ricci flows on surfaces. *J. Differential Geom.*, 63(1):97–129, 2003.
- [14] David Coulson, Oliver A. Goodman, Craig D. Hodgson, and Walter D. Neumann. Computing arithmetic invariants of 3-manifolds. *Experiment. Math.*, 9(1):127–152, 2000.
- [15] Raquel Díaz. Non-convexity of the space of dihedral angles of hyperbolic polyhedra. *C. R. Acad. Sci. Paris Sér. I Math.*, 325(9):993–998, 1997.
- [16] Raquel Díaz. A generalization of Andreev's theorem. *J. Math. Soc. Japan*, 58(2):333–349, 2006.
- [17] Anne Garrison and Richard Scott. Small covers of the dodecahedron and the 120-cell. *Proc. Amer. Math. Soc.*, 131(3):963–971 (electronic), 2003.
- [18] O. A. Goodman, C. D. Hodgson, and Neumann w. D. “snap home page”. See <http://www.ms.unimelb.edu.au/~snap>. Includes source distribution and extensive tables of results of Snap computations.

- [19] François Guéritaud. On an elementary proof of Rivin's characterization of convex ideal hyperbolic polyhedra by their dihedral angles. *Geom. Dedicata*, 108:111–124, 2004.
- [20] Poincaré Henri. Mémoire sur les groupes kleinéens. *Acta Math*, 3:49–92, 1883.
- [21] C. D. Hodgson. Deduction of Andreev's theorem from Rivin's characterization of convex hyperbolic polyhedra. In *Topology 90*, pages 185–193. de Gruyter, 1992.
- [22] Craig D. Hodgson and Jeffrey R. Weeks. Symmetries, isometries and length spectra of closed hyperbolic three-manifolds. *Experiment. Math.*, 3(4):261–274, 1994.
- [23] John H. Hubbard and Peter Papadopol. Newton's method applied to two quadratic equations in \mathbb{C}^2 viewed as a global dynamical system. To appear in the Memoires of the AMS.
- [24] John Hamal Hubbard and Barbara Burke Hubbard. *Vector calculus, linear algebra, and differential forms*. Prentice Hall Inc., Upper Saddle River, NJ, 1999. A unified approach.
- [25] Roland K. W. Roeder John H. Hubbard and William D. Dunbar. Andreev's theorem on hyperbolic polyhedra. To appear *Les Annales de l'Institute Fourier*.
- [26] Kaiki Taro Inoue. Numerical study of length spectra and low-lying eigenvalue spectra of compact hyperbolic 3-manifolds. *Classical Quantum Gravity*, 18(4):629–652, 2001.
- [27] L. V. Kantorovič. On Newton's method. *Trudy Mat. Inst. Steklov.*, 28:104–144, 1949.
- [28] Ruth Kellerhals. On the volume of hyperbolic polyhedra. *Math. Ann.*, 285(4):541–569, 1989.
- [29] F. Löbell. Beispiele geschlossener dreidimensionaler clifford-kleinische räume negativer krümmung. *Ber. Sächs. Akad. Wiss.*, 83:168–174, 1931.
- [30] A. Marden and B. Rodin. On Thurston's formulation and proof of Andreev's Theorem. In *Computational Methods and Function Theory*, volume 1435 of *Lecture Notes in Mathematics*, pages 103–115. Springer-Verlag, 1990.
- [31] G. A. Margulis. Certain applications of ergodic theory to the investigation of manifolds of negative curvature. *Functional Anal. Appl.*, 3(4):335–336, 1969.
- [32] A. D. Mednykh. Three-dimensional hyperelliptic manifolds. *Ann. Global Anal. Geom.*, 8(1):13–19, 1990.
- [33] Alexander Mednykh and Marco Reni. Twofold unbranched coverings of genus two 3-manifolds are hyperelliptic. *Israel J. Math.*, 123:149–155, 2001.
- [34] Alexander Mednykh, Marco Reni, Andrei Vesnin, and Bruno Zimmermann. Three-fold coverings and hyperelliptic manifolds: a three-dimensional version of a result of Accola. *Rend. Istit. Mat. Univ. Trieste*, 32(suppl. 1):181–191 (2002), 2001. Dedicated to the memory of Marco Reni.
- [35] Alexander Mednykh and Andrei Vesnin. Colourings of polyhedra and hyperelliptic 3-manifolds. In *Recent advances in group theory and low-dimensional topology (Pusan, 2000)*, volume 27 of *Res. Exp. Math.*, pages 123–131. Heldermann, Lemgo, 2003.
- [36] Marco Reni. Dihedral branched coverings of hyperbolic orbifolds. *Geom. Dedicata*, 67(3):271–283, 1997.
- [37] I. Rivin and C. D. Hodgson. A characterization of compact convex polyhedra in hyperbolic 3-space. *Invent. Math.*, 111:77–111, 1993.

- [38] Igor Rivin. On geometry of convex ideal polyhedra in hyperbolic 3-space. *Topology*, 32(1):87–92, 1993.
- [39] Igor Rivin. A characterization of ideal polyhedra in hyperbolic 3-space. *Ann. of Math. (2)*, 143(1):51–70, 1996.
- [40] Roland K. W. Roeder. A degenerate newton’s map in two complex variables: linking with currents. To appear J. Geometric Analysis.
- [41] Roland K. W. Roeder. Le théorème d’andreev sur polyèdres hyperboliques. Doctoral thesis (In English), May 2004. Université de Provence, Aix-Marseille 1.
- [42] Roland K. W. Roeder. Compact hyperbolic tetrahedra with non-obtuse dihedral angles. *Publicacions Matemàtiques*, 50(1):211–227, 2006.
- [43] J.-M. Schlenker. Dihedral angles of convex polyhedra. *Discrete Comput. Geom.*, 23(3):409–417, 2000.
- [44] Jean-Marc Schlenker. Métriques sur les polyèdres hyperboliques convexes. *J. Differential Geom.*, 48(2):323–405, 1998.
- [45] Jean-Marc Schlenker. Hyperbolic manifolds with convex boundary. *Invent. Math.*, 163(1):109–169, 2006.
- [46] M. Shub and S. Smale. Complexity of Bezout’s theorem. II. Volumes and probabilities. In *Computational algebraic geometry (Nice, 1992)*, volume 109 of *Progr. Math.*, pages 267–285. Birkhäuser Boston, Boston, MA, 1993.
- [47] Michael Shub and Steve Smale. Complexity of Bézout’s theorem. I. Geometric aspects. *J. Amer. Math. Soc.*, 6(2):459–501, 1993.
- [48] Michael Shub and Steve Smale. Complexity of Bezout’s theorem. III. Condition number and packing. *J. Complexity*, 9(1):4–14, 1993. Festschrift for Joseph F. Traub, Part I.
- [49] Michael Shub and Steve Smale. Complexity of Bezout’s theorem. IV. Probability of success; extensions. *SIAM J. Numer. Anal.*, 33(1):128–148, 1996.
- [50] Ken Stephenson. ‘CirclePack’. See <http://www.math.utk.edu/~kens/CirclePack/>.
- [51] W. P. Thurston. *The Geometry and Topology of 3-manifolds*. Princeton University Notes, Princeton, New Jersey, 1980.
- [52] Andrei Vesnin. Three-dimensional hyperbolic manifolds of Löbell type. *Siberian Math. J.*, 28(5):731–733, 1987.
- [53] Andrei Vesnin. Volumes of Löbell 3-manifolds. *Math. Notes*, 64(1-2):15–19, 1998.
- [54] È. B. Vinberg. Discrete groups generated by reflections in Lobačevskiĭ spaces. *Mat. Sb. (N.S.)*, 72(114):471–488; correction, ibid. 73 (115) (1967), 303, 1967.
- [55] È. B. Vinberg. Hyperbolic groups of reflections. *Russian Math. Surveys*, 40(1):31–75, 1985.
- [56] È. B. Vinberg. The volume of polyhedra on a sphere and in Lobachevsky space. In *Algebra and analysis (Kemerovo, 1988)*, volume 148 of *Amer. Math. Soc. Transl. Ser. 2*, pages 15–27. Amer. Math. Soc., Providence, RI, 1991.
- [57] È. B. Vinberg and O. V. Shvartsman. Discrete groups of motions of spaces of constant curvature. In *Geometry, II*, volume 29 of *Encyclopaedia Math. Sci.*, pages 139–248. Springer, Berlin, 1993.
- [58] J. R. Weeks. “SnapPea”. See <http://geometrygames.org/SnapPea/index.html>.